INTERNATIONAL SCIENTIFIC JOURNAL

trans & MOTAUTO WORLD

ISSN PRINT 2367-8399
ISSN WEB 2534-8493

YEAR V, ISSUE 1/2020





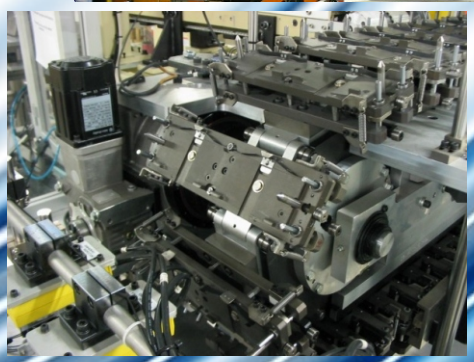



SCIENTIFIC TECHNICAL UNION OF MECHANICAL INGENEERING "INDUSTRY 4.0"
108 RAKOVSKI STR., SOFIA 1000, BULGARIA

INTERNATIONAL SCIENTIFIC JOURNAL

TRANS MOTAUTO WORLD

PUBLISHER:

SCIENTIFIC TECHNICAL UNION OF MECHANICAL ENGINEERING INDUSTRY-4.0

108, Rakovski Str., 1000 Sofia, Bulgaria
tel. (+359 2) 987 72 90,
tel./fax (+359 2) 986 22 40**,**
office@stumejournals.com
www.stumejournals.com

ISSN PRINT 2367-8399
ISSN WEB 2534-8493
YEAR V, ISSUE 1 / 2020

EDITORIAL BOARD

CHIEF EDITOR
Prof. Petar Kolev, Bulgaria

MEMBERS:

Prof. Ahmet H. Ertas, TR
Prof. Aleksandar Kostikj, MK
Prof. Andrey Ferenets, RU
Prof. Angel Dimitrov, BG
Prof. Beti Angelevska, MK
Prof. Dainis Berjoza, LV
Prof. Dan Scarpete, RO
Prof. Daniela Todorova, BG
Prof. Emilia Andreeva-Moschen, AT
Prof. Gordana Marunic, HR
Prof. Hristo Stanchev, BG
Prof. Igor Penkov, EE
Prof. Igor Smirnov, UA
Prof. Igor Taratorkin, RU
Prof. Iliyan Lilov, BG
Prof. Lech Sitnik, PL
Prof. Ljudmila Boyko, UA
Prof. Madaminjon Aripdzanov, UZ
Prof. Martin Kendra, SK
Prof. Massimo Borghi, IT
Prof. Miho Mihow, BG
Prof. Murat Dogruel, TR
Prof. Natalia Sidenko, LV
Prof. Natasa Tomic-Petrovic, RS
Prof. Nikolay Georgiev, BG
Prof. Nikolay Ovchenkov, RU
Prof. Oleg Sharkov, RU
Prof. Pepo Yordanov, BG
Prof. Polatbeg Zhunisbekov, KZ
Prof. Rinat Kurmaev, RU
Prof. Rosen Ivanov, BG
Prof. Teymuraz Kochadze, GE
Prof. Tomaz Morchadze, GE
Prof. Vadim Zhmud, RU
Prof. Valyo Nikolov, BG
Prof. Zoran Jovanovic, RS

RESPONSIBLE SECRETARY:
Prof. Nikolay Tonchev, Bulgaria

C O N T E N T S

TRANSPORT TECHNICS. INVESTIGATION OF ELEMENTS. RELIABILITY

Advantages of using composite materials in automotive manufacture process
Štefan Kender, Janette Brezinová, Henrich Sailer 3

On Electromagnetic Actuator Control in The Active Suspension Systems
Katerina Hyniova 6

Some approaches to the non-destructive control of composite materials used in the aerospace industry
Valeri Panevski 9

TRANSPORT. SAFETY AND ECOLOGY. LOGISTICS AND MANAGEMENT

Size and speed of data generated by Fleet Management Software
Nikolay Kaskatiiski 13

Analysis of the causes that generate traffic accidents
Angela Popusoi 17

Geometric parameters in railroad crossing based reconstruction of Iliantsi-Curilo and Curilo-Rebrovo
Vladimir Popov 20

Researching of the factors determinant safety movement of the train in braking regime – impact of braking force on the superstructure of the railway with regard to the interoperability and the experience of the railway section Gorna Oriahovitsa
Kina Kutsarova-Dimitrova 23

VEHICLE ENGINES. APPLICATION OF FUELS TYPES. EFFICIENCY

The change in energy flow streams for main marine propulsion steam turbine at different loads
Mrzljak Vedran, Prpić-Oršić Jasna, Medica-Viola Vedran, Anđelić Nikola 26

Methodology for static tuning of the HEV fuel flow measuring system
Slavcho Bozhkov, Georgi Tonkov 30

Investigation of the influence of fulleren-containing oils on tribotechnical characteristics
Derkach Oleksii, Kobets Anatolii, Aulin Viktor, Kabat Oleh, Makarenko Dmytro, Hrynkiv Andriy, Shchus Bogdan 34

Advantages of using composite materials in automotive manufacture process

Štefan Kender[1], Janette Brezinová[1], Henrich Sailer[1]
Faculty of Mechanical Engineering, Technical university of Kosice, Slovakia[1]
stefan.kender@tuke.sk

Abstract: *The advantages of using composite materials are currently manifested in various industries. This creates space for their even greater application in the automotive industry. Car manufacturers strive to constantly reduce the weight of the car, increasing its durability and safety at the same time. Car consumption and associated emissions are closely monitored. Composite materials therefore offer a range of properties that meet today's automotive requirements to a large extent.*
Keywords*: COMPOSITE MATERIAL, AUTOMOBILE PRODUCTION, CARBON FIBERS, APPLICATION*

1. Introduction

Composites are materials created by combining existing materials and using the knowledge of physical metallurgy. They consist of at least two components. The first continuous component - the matrix - serves as a binder, the secondary discontinuous component (disperse particles, fibers or layers) has a reinforcing function. They have excellent mechanical properties and have therefore started to be applied in all industries. The main disadvantage of composites is their high price and demanding production. Composites in the automotive industry were first used in motorsport. At present, composite materials are applied not only in sports and luxury cars but also in mass-produced vehicles. Automotive manufacturers are working to reduce weight and emissions, and increase the safety and durability of cars. For this reason, they cooperate with manufacturers of composite materials who have many years of experience with the extensive use of composites. Together, they are trying to find a suitable technology that will make the production of composite parts easier, cheaper and faster. The production of composite structures for the automotive industry is the most advanced new market and their use in the production of automotive components has a very great future.

2. Materials for Production of Prototype Parts

The use of composites in automotive production is mainly based on the effort to replace steel and other metallic materials, reduce weight, increase strength, durability, etc. Composite components have excellent properties that cannot be achieved with other materials.

In the early 1990s, the use of modern composite materials caused a revolution in the world's automotive engineering. In 1984, McLaren produced the monocoque of his F1 vehicle from carbon fiber. At present, the use of composites is more or less the norm, especially for sports cars.

Composites advantages:

- fatigue resistance,
- high strength and modulus of elasticity,
- resistance against crack propagation,
- high collision and notch toughness,
- resistance to fire,
- vibrations absorbing ability,
- surface quality,
- corrosion resistance,
- ballistic proprieties,
- electrical conductivity,
- renewable usability. [2]

Main disadvantage of the composites is their high price and difficult production. Main reasons for using the composites materials in car production are:

- decreasing of the car weight,
- decreasing of the car fuel consumption,
- increasing of the safety and the impact strength,
- renewable usability. [2]

Table 1: *Mechanical properties of metallic and composite materials comparison [4].*

Material	Specific mass ($g.cm^{-3}$)	Tensile strength (MPa)	Modulus of elasticity of tensile E(GPa)	Specific strength (N.m/kg)
Steel	7.8	1300	200	167
Aluminum	2.81	350	73	124
Titan	4	900	108	204
Magnesium	1.8	270	45	150
Fiberglass	2.10	1100	75	524
Aramid	1.32	1400	45	1060
IM Carbon	1.51	2500	151	1656
HM Carbon	1.54	1550	212	138

Weight reduction and reduction of vehicle consumption

Through weight reduction the fuel consumption may also be decreasing. By the 10% weight decreasing, the fuel consumption is circa 7% decreasing, what also means that reducing the weight by about 1kg will measurable reduce the CO_2 emissions. [3]

Automotive manufacturers are working to reduce greenhouse gas emissions by using new ultralight materials. The only obstacle to the use of such materials is their high price, which is why great emphasis is placed on the development of new technologies and production processes.

Table 2: *Decreasing of the consumption by the car weight reduction [3]*

Design/ Engine type	Car weight	Fuel consumption (l/100 km)	Increasing of the fuel efficiency
Basic state	500 kg	10	0 %
A) High strength steel	350 kg (30%)	9.58	4.20 %
B) Carbon composites structure	270 kg (42%)	9.31	7 %

C1) Diesel engine		7	30 %
C2) Full hybrid(Otto)		6.5	35 %
C3) Full hybrid (Diesel)		5.5	45 %

As the figure shows, against of the new materials application, the weight of modern cars isn´t much different from the cars from the 70 s. Of course, this isn't caused only by false of materials, but "weight problem" of the cars can be in the future solved with intensive using of composite materials. [4]

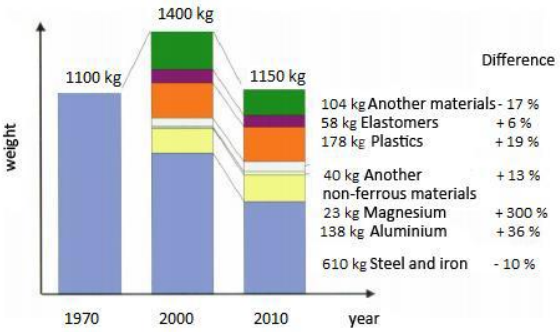

Fig. 1 *Working principle of 3D the printer EOSINT M 2701.*

Increasing safety and impact resistance

The impact strength is an ability of the material structure to absorb the energy through a controlled way. The demands for car impact strength are:

- Deformable end section of the car, which preserve the integrity of the back passenger space and protect the fuel tank.
- Right designed the side structure and the doors.
- Strength roof construction, that protect by the turnover.
- Properly designed interior space.

Composite materials have great ability to absorb the energy. They are made up from layers that are absorbing the impact energy by the separating process. The ability of the energy absorbing is shown on the next figure. (Fig. 2).

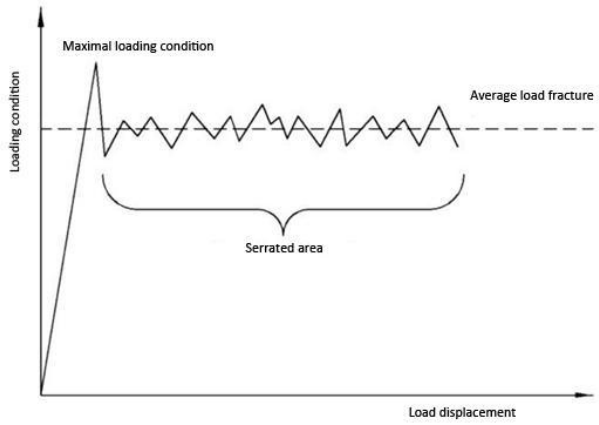

Fig. 2 Graph of the impact energy absorbing [5].

Through the energy absorbing testing, there are developing variously kinds of the surface damages.

We know 3 types of composite materials damage::

a) The fibres disruption.

b) Fragmentation.

c) Brittle fracture.

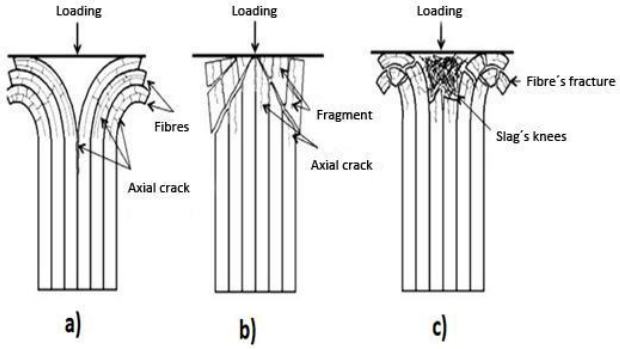

Fig. 3 The types of material damages: - a) The fibres disruption b) Fragmentation c) Brittle fracture [5].

We can present the ability of absorbing the impact energy by the SEA parameter (Specific Energy of Absorption). SEA is J/g and for composite materials is at intervals of 15-80 J/g. [6]

We can get SEA as:

$$SEA = \frac{EA}{\rho . A . l}$$

EA - Energy Absorbed.

A – Cross-section of the sample.

ρ – Density.

l - Length of the energy absorbing.

We can get EA from the graph of the impact energy absorbing:

$$EA = \int F . dl$$

F – Immediate strength of the crush.

As we can see on figure 4, the composite materials have a great ability to absorb the impact energy in comparison to metal materials.

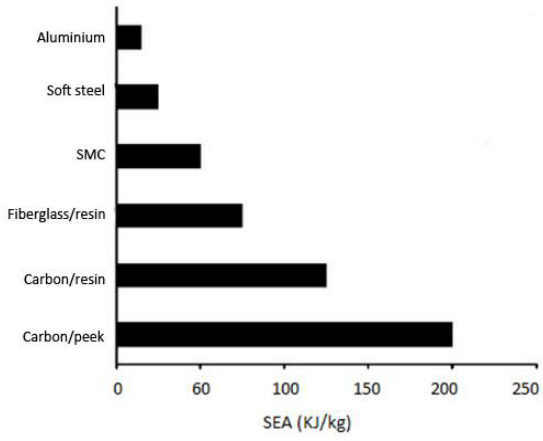

Fig. 4 The energy absorbtion of specific materials [3].

The use of composite materials in car construction was also included in the project of a student prototype car with the working name ICAR, which was implemented at the Faculty of Mechanical Engineering of the Technical University in Košice. Students

designed the car's body and interior. The production of the body was carried out using carbon fibers. The car was built on the chassis of the Škoda Fabia 1.9 TDI and is fully functional. It achieves excellent driving characteristics, because the use of composite materials has significantly reduced the weight of the car. In addition, it has a modified chassis, reduced center of gravity and computer-modified engine parameters. All body parts, including some interior elements, were made of composite materials. It was a very large project involving 25 engineering students. When solving individual tasks, they got acquainted with the whole process from the design of the car to the actual implementation of the production of a functional prototype of the car. They verified on a real project the advantages of using composite materials in the construction of a car and their overall contribution, which was reflected in the driving characteristics of the ICAR car.



Fig. 5 Prototype ICAR.



Fig. 6 Interior prototype ICAR.

3. Conclusion

The use of new materials such as composites allow designers to design different shapes of components that can be applied in automobiles. The design of modern cars affects safety, performance, aerodynamics, car consumption, production costs and many other important factors. Likewise, composite materials are used to improve the appearance of exteriors or interiors, such as. seats, dashboards, wings, bumpers, etc. Research is currently underway and various studies are underway on conventional all-carbon cars. The advantages of using composite materials in automotive production will therefore become more and more important and the scope for their application will be constantly expanding.

Acknowledgments: This work was supported by scientific grant agency of the Ministry of Education of the Slovak Republic VEGA No. 1/0497/20, KEGA 001STU-4/2019 and of the Slovak Research and Development Agency APVV-16-0359.

4. References

1. Composite Materials in Automotive Engineering. [online]. [cit. 16.06.2017]. http://www.thinkengineering.net/104/composite-materials-in-automotive-engineering/automotive-engineering/

2. České vysoké učení technické v Prahe – Plasty a kompozity. [online]. [cit. 23.08.2018]. http://www.mmspektrum.com/clanek/plasty-a-kompozity-naplnuji-materialove-pozadavky-moderniho-strojirens.html

3. University Visvesvaraya College of Engineering - A seminar on:Applications of Composite materials in the Automobile industry. [online]. [cit. 18.08.2018]. http://www.scribd.com/doc/32475280/Composites-in-the-Automobile-Industry

4. University of Sheffield – Materials in Utomotive application,State of the Art and Prospects. [online]. [cit. 18.08.2018]. http://cdn.intechopen.com/pdfs/13343/InTech-Materials_in_automotive_application_state_of_the_art_and_prospects.pdf

5. D. Adams: Testing the crashworthiness of composite structures. [online]. [cit. 20.10.2018]. http://www.compositesworld.com/articles/testing-the-crashworthiness-of-composite-structures

6. P. Freabolli, et al.: Efforts in the Standardization of Composite Materials Crasshworthiness Energy Absorption. [online]. [cit. 12.10.2018]. http://www.aa.washington.edu/research/structures/pubs/211%20small.pdf

7. M. Dúbravčík, Š Kender: Composite materials application in car production. Transfer inovácií č. 29 (2014), s. 282-285. - ISSN 1337-7094. http://www.sjf.tuke.sk/transferinovacii/pages/archiv/transfer/29-2014/pdf/282-285.pdf

8. G. Savage : Composite Materials Technology in Formula 1 Motor Racing. [online]. [cit. 18.12 2018]. http://www.speautomotive.com/SPEA_CD/SPEA2008/pdf/k/K3.pdf

9. W. Papacz, E. Tertel, P. Kurylo: Performance comparison of conventional and composite leaf spring. In. Journal of Measurements in Engineering. 2014, Vol. 2, no. 1, s. 24--28

10. Why Raw Composite Material Prices Increas [online]. [cit. 24.06.2018]. Dostupné na internete: http://composite.about.com/od/materialsanddistributors/a/Why-Raw-Composite-Material-Prices-Increase.html

On electromagnetic actuator control in the active suspension systems

Katerina Hyniova
Faculty of Information Technology
Czech Technical University in Prague, Prague, Czech Republic
hyniova@fit.cvut.cz

Abstract: *In the paper, the design of a linear motor as an actuator in vehicle active suspension systems will be presented. The attention is focused on several interesting design aspects of a non-traditional actuator (a linear synchronous permanent magnet motor with electronic commutation) controlled to obtain a variable mechanical force for a car active suspension. The main advantage of such a solution is the possibility to generate desired forces acting between the unsprung (wheel) and sprung (car body) masses of the car, providing good insulation of the car sprung mass from the road surface disturbances. In addition, under certain circumstances it is possible to reduce or even eliminate the demands concerning the external power source.*
Keywords*: CONTROL, VEHICLE, LINEAR MOTOR, SUSPENSION*

1. Introduction

All suspension systems are designed to meet specific requirements. In suspension systems, usually two most important features are expected to be improved - disturbance absorbing (i.e. passenger comfort) and attenuation of the disturbance transfer to the road (i.e. car handling). The first requirement could be presented as an attenuation of the damped mass acceleration or as a peak minimization of the damped mass vertical displacement. The second one is characterized as an attenuation of the force acting on the road or in a simple car model (Fig.1) as an attenuation of the unsprung mass acceleration. It is obvious, that there is a contradiction between these two requirements. With respect to these contradictory requirements, the best results can be achieved using active suspension systems generating a variable mechanical force acting in the system.

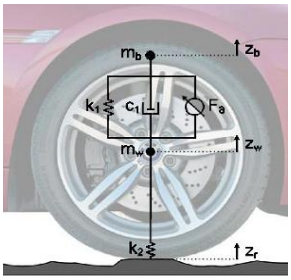

Fig. 1 *One-quarter-car suspension model*

The model consists of a spring (stiffness k_1), passive damper (damping quotient c_1), sprung mass is taken as one-quarter of the body mass (m_b), unsprung mass representing one wheel (m_w) and a spring connecting the unsprung mass to the road and representing the tire stiffness (k_2), $z_r(t)$ is road displacement (road disturbance) [m], $z_b(t)$ denotes displacement of the sprung mass, and $z_w(t)$ displacement of the unsprung mass.

The active force (F_a) acting between the sprung and unsprung masses of the car is generated by a linear electric motor. For one-quarter-car model description see [1]. The H∞ controller synthesis for active suspension is described in [2].

The paper offers motivations for an electromagnetic active suspension system that provides both additional stability by performing active roll and pitch control during cornering and braking, as well as eliminating road irregularities, hence increasing both vehicle and passenger safety and driving comfort. Contrary to the conventional suspension system, a quite non-traditional solution has been chosen [1], [2] . In the paper, the usage of linear motors as electromagnetic actuators in the vehicle active suspension systems is presented. Vehicle suspensions in which forces are generated in response to feedback signals by active elements offer increased design flexibility compared to the conventional suspensions using passive elements such as springs and dampers. The attention is concentrated on several aspects of such a non-traditional actuator controlled to obtain a variable mechanical force for the car suspension. The main advantage of such a solution is the possibility to generate desired forces acting between the unsprung (wheel) and sprung (car body) masses of the car, providing good insulation of the car sprung mass from the road surface and load disturbances. Besides, under certain circumstances using linear motors as actuators enable the transformation of mechanical energy of vibrations to electrical energy, the energy accumulation, and using it when needed. This way, it is possible to reduce or even eliminate the demands concerning the external power source. The active suspension offers many benefits over conventional and semi-active suspension systems. The electromagnetic suspension is a high bandwidth and efficient solution for improving handling and comfort. Direct drive tubular permanent magnet actuator technology offers a high force density and fail-safe solution. In-lab and simulation verification proved the performance and efficiency of the proposed solution. Compared to traditional drives that use rotational electro motors and lead screw or toothed belts, the direct-drive linear motor exhibits the property of contactless transfer of electrical power according to the laws of magnetic induction. The electromagnetic force is applied directly without the intervention of a mechanical transmission. Low friction and no backlash resulting in high accuracy, high acceleration and velocity, high force, high reliability and long lifetime enable not only effective usage of modern control systems but also represent the important attributes needed to control vibration suspension efficiently.

2. Linear Motors

The beauty of linear motors is that they directly translate electrical energy into usable linear mechanical force and motion, and vice versa. The motors are produced in synchronous and asynchronous versions. Compared to conventional rotational electro motors, the stator and the shaft (translator) of direct-drive linear motors are linear-shaped. One can imagine such a motor taking infinite stator diameter.

Linear motor translator movements take place with high velocities (up to approximately 200m/min), large accelerations (up to g multiples), and forces (up to kN). As mentioned above, the electromagnetic force can be applied directly to the payload without the intervention of a mechanical transmission, what results in high rigidity of the whole system, its higher reliability and longer lifetime. In practice, the most often used type is the synchronous three-phase linear motor.

For the most part, linear motors function within a system in the same manner as other types of motors. The major difference lies in commutation. Linear motors commutate based on linear position; rotary motors commutate based on angular position.

For a brushless motor to produce force, the windings must be switched in polarity and amplitude relative to the permanent magnetic field. In the case of brush-type motors, the magnets are usually stationary (stator). In brushless motors, the magnets are typically on the moving shaft, either rotating or sliding. Commutation is cyclical in nature, and is based on a fixed ratio of magnetic poles to electric coils. With rotary motors, these cycles repeat every revolution. With linear motors, the cycles repeat over a fixed distance.

3. Accumulation of Energy

Linear electric motors are able to recuperate energy. When the generated force is of the same direction as the suspension velocity, the energy has to be supplied into the system. Otherwise, it can be recuperated and accumulated for future usage.

Assume two driving conditions:

- the terrain/surface the car is driving on is very rough and uneven and there is enough energy stored in the accumulator system (the controller works in the standard mode, the motor consumes energy from the energy accumulator (supercapacitors) and the suspension performance is preserved).
- the terrain/surface the car is driving on is relatively smooth and there is not enough energy stored in the accumulator system because of the situation described above. The external signal provides the information to the H∞ controller to deteriorate its performance and to reduce energy consumption [2]. The deterioration is stated by the desired force attenuation. If the force is attenuated too much then the active suspension system works similarly to the passive suspension and the linear electric motor works as a generator producing energy for the accumulation system (Fig.2). Of course, in such a case the suspension performance is deteriorated (to the passive suspension level in the worst case).

The power amplifier requires a DC power supply for the switch bridge (see Fig.2a). If the motor works as an actuator, the electrical energy is lead in the terminal U_0. In the braking mode, it is possible to get back the accumulated energy from the terminal. To achieve a good function of the power amplifier, the level of the voltage U_0 cannot exceed a permitted range. Because the maximum of the linear motor force is limited within the given permitted range, it is useful to hold U_0 at the upper limit. There are several ways of energy accumulation, but some of them do not allow holding U_0 at the upper limit of the range. One of the possibilities is shown in Fig.1a. U_0 is held constant and equal to U_{max}.

The electrical energy is impressed across the terminal U_0 from vehicle supply network here represented by the capacitor C with the help of a DC/DC step-up converter. The voltage of the capacitor C is held within the range of $0 \div U_{max}$ [V]. With respect to the short-time (hundreds of ms) instantaneous power (of the order of kW), both the converters have to be adjusted to such a high peak power. Consider the average efficiency of each converter as equal to η=0,85. The recuperated energy can be reused with the efficiency of η^2=0,72. It results in a disadvantage when 28% of the recuperated energy is lost during one cycle of the energy accumulation and its following reusage.

If the vehicle supply network is represented by a capacitor C then its accumulation capacity (taken in the range of $(0\text{-}U_{max})$ enables to store energy of:

$$E_{C1} = \frac{1}{2} C U_{max}^2 \quad (1)$$

Another way how to accumulate the electrical energy is shown in Fig.1b. In this case, it is assumed that the voltage U_0 does not have to be necessarily time-invariant and varies within the range of U_{min} , U_{max} . Now, the capacitor C is connected directly to the terminal U_0 . The peak-power dimensioned auxiliary voltage supply is non-active for $U_0 > U_{min}$. Vice-versa, the energy dissipator dissipates energy in case of exposure of the capacitor when $U_0 > U_{max}$. The main advantages of such a solution are: its simplicity, the fact that the energy taken from the terminal U_0 is stored with the efficiency of 100% (loss resistance of the capacitor C is neglected), and no problems concerning the DC/DC converters (efficiency, disturbances, cooling etc.). As the main disadvantage is taken the fact that the stored energy is limited by:

$$E_{C2} = \frac{1}{2} C (U_{max}^2 - (U_{min}^2) \quad (2)$$

To store the same energy as in the first case, it is necessary to use the capacitor with E_{C1}/E_{c2}- times higher capacity.

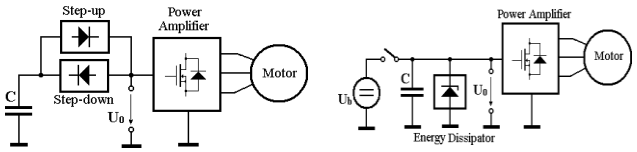

Fig. 2a,b *Energy accumulation.*

4. Linear Motor Model

To verify control algorithms a linear motor model including the power amplifier has been created in Matlab-Simulink. The model enables to demonstrate the conversion of the electrical energy to mechanical energy.

In the model, it is assumed that: the magnetic field of the secondary part with permanent magnets is sinusoidal, the phases of the primary part coils are star-connected, and the vector control method is used to control the phase current. Here, PWM voltage signal is substituted by its mean value to shorten (about 10 times) the simulation period (inaccuracies caused by such a substitution can be neglected). The principal inner representation of the model is shown in Fig.3. The model input vector is given by the instantaneous position [m] (necessary to compute the commutation current [A] of the coils), instantaneous velocity [m/s] (the induced voltage of the coils depends on the position and velocity) and desired force [N].

The designed model function has been verified comparing dynamics of the model and the real motor. The simulation parameters correspond to the catalogue parameters of TBX3810 linear motor manufactured by Thrust-tube. For example, time responses caused by changes of the desired force has been compared. The linear motor input-output model is shown in Fig.4.

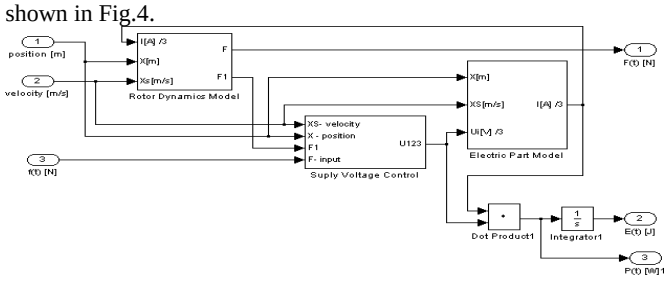

Fig. 3 *Principal inner model representation*

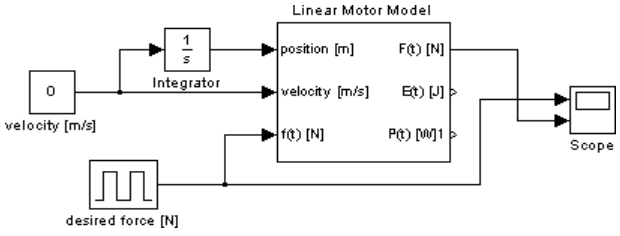

Fig. 4 *Linear motor input/output model for dynamics verification*

Fig. 5 and Fig.6 represent simulated and real time responses (step series: 0N→200N/200N→0N, power supply: 150V, velocity: 0m/s).

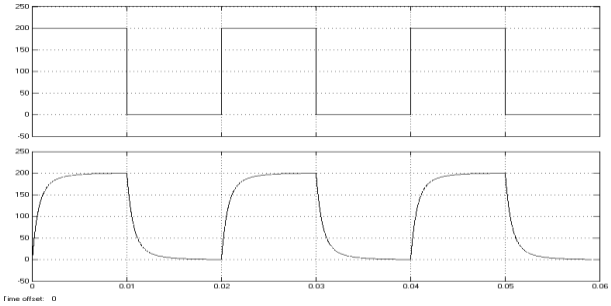

Fig. 5 Simulated time responses

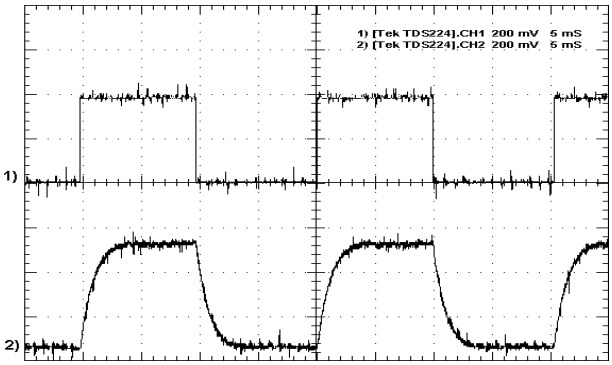

Fig. 6 *Real time responses*

On the base of the experiments taken on the suspension model, the value of the electric power necessary to be supplied or consumed when the velocity and force of the motor are constant has been gained. The model output vector is given by the actual value of the force [N], electric power [W] has been consumed at the switch bridge terminal since the start point of the simulation (its negative value represents the recuperated electrical energy), and instantaneous electric power demand of the motor [W]. In Fig.7 there is represented an input/output model (with concrete simulation values) of the linear motor.

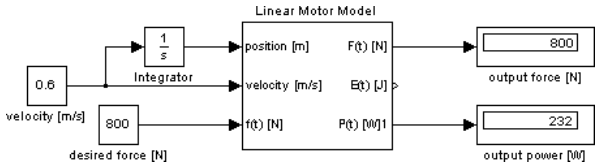

Fig. *7 Linear motor input-output model*

To obtain the simulation results given in Tab.1, the linear motor motion of constant velocity and constant force has been simulated (the results in Tab.1 are valid for the supply voltage of 300V).

The direction of the force is oriented contrariwise for positive values of the force. After transient response settling, the power supply of the linear motor (the power supplied into the motor from the power supply or vice versa) has been measured. The positive values correspond to the electric power necessary to be supplied to the motor. Vice versa, the negative values represent the accumulate-able power. xxxx symbols in the fields signify that the desired force is not reachable under the given velocity. The simulation parameters correspond to the catalogue parameters of TBX3810 linear motor Thrust-tube.

Acknowledgment

This research has been supported by MSMT project INTER-VECTOR 17019.

Table 1 *Simulation results*

velocity [m/s]								
force [N]	**0**	**0,1**	**0,2**	**0,6**	**1**	**1,2**	**1,5**	**2**
2000	4931	4693	4459	3991	3523	2591	1430	276
1800	3996	3780	3569	3148	2727	1889	846	**-191**
1600	3157	2965	2778	2404	2030	1286	360	**-556**
1400	2417	2249	2085	1758	1432	781	**-26**	**-828**
1200	1776	1632	1492	1211	932	376	**-315**	**-999**
1000	1233	114	967	763	531	68	**-504**	**-1071**
800	789	694	600	414	232	**-140**	**-595**	**-1044**
600	444	372	302	163	24	**-250**	**-587**	**-919**
400	197	150	103	11	**-81**	**-261**	**-481**	**-695**
200	49	26	3	**-43**	**-87**	**-173**	**-276**	**-372**
0	0	0	1	2	5	13	28	49
-200	49	74	98	146	196	298	430	567
-400	197	246	293	389	485	671	931	xxxxx
-600	444	516	587	730	873	1163	1531	xxxxx
-800	789	886	980	1170	1360	1744	2229	xxxxx
-1000	1233	1354	1471	1708	1946	2424	3026	xxxxx
-1200	1776	1920	2062	2345	2630	3202	xxxxx	xxxxx
-1400	2417	2585	2750	3081	3413	4079	xxxxx	xxxxx
-1600	3157	3349	3538	3916	4294	xxxxx	xxxxx	xxxxx
-1800	3996	4212	4424	4849	5274	xxxxx	xxxxx	xxxxx
-2000	4931	5173	5405	5876	xxxxx	xxxxx	xxxxx	xxxxx

5. Results

Comparing the time responses in Fig.5 and Fig.6 it can bee seen a very good matching level of the behavior of the used model and real motor.

On the base of the simulation results, it is obvious that the power of the order of up to hundreds of W can be obtained when the motor velocity exceeds 0,4 ms^{-1} and the force does not exceed about 200N. As an example, it is possible to note that under the motor velocity of 1,5 ms^{-1} the energy can be obtained if and only if the braking force does not exceed 1400N.

6. Conclusion

It results from the experiments made with the linear motor TBX3810 Thrust-tube that the designed model describes the real linear motor equipped with necessary auxiliary circuits very authentically and enables to verify control algorithms developed to control the linear motor as an actuator of the active suspension system. This was an important conclusion for controller synthesis, various experimental simulations, and further research.

References

[1] Hyniova, K., J. Honcu, A. Stribrsky: Vibration Control in Suspension Systems, in Proceedings of 16th World Congress of the International Federation of Automatic Control, Prague, Czech Republic, pp.176-182,(2005)

[2] Kruczek, A., K. Hyniova, A. Stribrsky: H∞ Control of Automotive Active Suspension with Linear Motor“, in Proceedings of 3rd IFAC Symposium on Mechatronic Systems, Sydney, Australia, (2004)

[3] Zhou, K., J. C. Doyle, Essentials of Robust Control, Prentice Hall, USA,(1998)

Some approaches to the non-destructive control of composite materials used in the aerospace industry

Valeri Panevski
Bulgarian Academy of Sciences, Institute of Metal Science Equipment and Technologies with Hydro- and Aaerodynamics Centre "Acad. A Balevski", Sofia, Bulgaria
panevski@ims.bas.bg

Abstract: *One of the priority areas for the use of composite materials is the aerospace industry. A number of evaluations have shown that their use in the manufacture of modern aircraft and helicopters lead to a reduction in weight of the respective parts with 20-30% compared to the same manufactured from conventional materials. In this case, an increase in the resistance of the respective part to external influences is usually achieved, and in many cases a decrease in its production cost.*

The increasing use of composite materials in the aerospace industry requires analyzing options for their diagnosis and non-destructive examination of their quality, taking into account their specific features. Because of the enormous diversity and complexity composition for composite materials, various methods of diagnosis have different efficiencies for different types of composites. In many cases, composites contain highly porous or fibrous layers, which results in a strong attenuation of the acoustic waves and render the acoustic method inapplicable to their non-destructive control. In these and other cases, the use of emerging methods for their non-destructive ultra-high frequency (microwave) diagnostics is of interest.

Keywords*: COMPOSITE MATERIALS; NON DESTRUCTIVE CONTROL*

1. Introduction

Composite materials are known to consist of two or more materials with different physical or chemical properties, which together form a composite with properties other than their own. In most cases, composites are created to give them better opportunities for use in various mechanical impacts (friction, shock, vibration, acceleration, loading, etc.), the temperature characteristics of the environment in which they function (extreme or rapidly changing over a wide range of temperatures), chemical and electromagnetic parameters of the environment in which they function (salinity, acidity, radiation, etc.), as well as to achieve certain physicochemical parameters at less weight or with smaller production costs and **[1-4]**.

One of the priority areas for the use of composite materials is the aerospace industry. A number of evaluations have shown that their use in the manufacture of modern aircraft and helicopters lead to a reduction in weight of the respective parts with 20-30% compared to the same manufactured from conventional materials. In this case, an increase in the resistance of the respective part to external influences is usually achieved, and in many cases a decrease in its production cost.

2. Composite materials

In the aerospace industry, composites have been used mainly in the military aircraft industry, but have recently become more widely used in the development of commercial aircraft. The advantages of using composites over traditional aluminum alloys are many, which is why they are more widely used. For the most part, the composite materials used in the aerospace industry are made of two major fiber and matrix components. Fibers or reinforcement provide high strength and hardness, while the matrix is used to bind the fibers together.

Another approach in the construction of composite structures is the layered structures (laminates), which can be made of different types of fiber composites oriented in different directions for optimum strength and rigidity.

An important type of laminated composite is the sandwich composite (a very lightweight but still robust composite laminate), which consists of a lightweight base panel with thin sheets of solid material bonded to the two faces of the core.

The increasing use of composite materials in the aerospace industry imposes the requirement to analyze the possibilities for their diagnosis and non-destructive examination of their quality, taking into account their specific features. Because of the huge variety and complex composition of composite materials, various methods of diagnosis have different efficiencies for different types of composites **[5-7]**.

In many cases, composites contain highly porous or fibrous layers, which results in a strong attenuation of the acoustic waves and render the acoustic method inapplicable to their non-destructive control.

The most famous example of the relevance and significance of this problem is the space shuttle crash of Space Shuttle Columbia in 2003. According to NASA experts, published in the authoritative edition of Aviation Week & Space Technology, one of the reasons that led to the crash were defects in the thermal insulation of the outer fuel container of the spacecraft. This insulation layer is a polyurethane foam with a thickness of 2.5-5.0 cm, applied onto the outer surface of the container to reduce the boiling point of the cryogenic components of the fuel (liquid hydrogen and oxygen) on the launch pad.

During the preparation for the start, which lasted several days, the moisture from the air penetrated the crevices of the coating and due to the difference in temperatures condensed therein. According to one hypothesis, as the shuttle took off, as the flight altitude increased, the external pressure decreased rapidly, causing the water to boil explosively, creating increased pressure. This resulted in the removal of a layer of thermal insulation coating which was rejected from the air stream and caused damage to the leading part of the wing of the space vehicle. Upon landing, at the stage of entering the Earth's atmosphere, plasma penetrates the openings, causing complete destruction of the apparatus and causing the death of the entire crew. Several other similar incidents have been reported, both in the aerospace and energy fields, which fortunately did not lead to such distressful consequences.

Therefore, the non-destructive diagnostics of composite materials of this type requires the development of new technologies, one of which could be the proposed technology of radar ultra-high frequency radiation in the GHz range. In these and other cases, the use of emerging methods for their non-destructive ultra-high frequency (microwave) diagnostics is of interest.

In general, the objectives of microwave diagnostics can be classified as superficial diagnosis - for the presence of superficial heterogeneities and / or defects, sub superficial diagnostics - for heterogeneities and / or defects within the composite material itself, and superficial diagnostics and for non-uniform defects. material behind the composite material or behind a certain layer of composite material.

3. Diagnosis methods

Depending on the method of diagnosis, it is appropriate that it be classified as a diagnosis on the basis of reflection (reflective diagnosis) or diagnosis on the basis of transition in the material (transient diagnosis).

Reflective diagnosis is more commonly used and is performed with the ultra-high frequency transmitter and receiver located on the same side of the material. In this case, the heterogeneity and / or the defect are recorded on the basis of the change in the signal received by it. Basically reflective surface diagnosis is applicable to all types of composite materials.

In the *transient diagnosis*, the transmitter and the receiver of the ultra-high frequency oscillation are located on both sides of the composite material, and inhomogeneities and / or defects are recorded based on the change of the signal passed through them.

In the case of composite materials whose surfaces are electrically conductive, a basic reflective ultra-high-frequency diagnosis is possible for the presence of surface inhomogeneities and / or defects. In some cases, when the electrically conductive surface layer is twice less than the penetration depth, a reflective diagnosis of the interior of the material is possible, and when this layer is less than the penetration depth, a transient diagnosis is also possible.

For matrix composite materials whose matrices are of electrically conductive material, but their reinforcement is of non-electrically conductive material, the possibilities for subsurface and subsurface ultra-high frequency diagnostics depend on the size and density of the matrix components. If the dimensions of the matrix component are significantly smaller than the depth of penetration of radiation into it, or if the distance between the individual individual components exceeds 0.25 - 0.5 of the length of radiation, it may be possible to perform sub-surface and even sub-surface reflective or transient diagnostics.

If the matrix and its reinforcement are not composed of conductive material, then it is possible to perform sub-surface and sub-surface ultra-high frequency reflective and transient diagnostics.

If the matrix is not composed of electrically conductive material but its reinforcement is of electrically conductive material, then in principle the possibilities of performing sub-surface and sub-surface ultra-high frequency diagnostics are extremely limited.

If the composite material is multilayered and the individual layers are not composed of conductive material, then there are possibilities for under-surface and sub-surface reflection and transient high-frequency diagnostics. If the composite material is multilayer, but only part of the individual layers (including the surface material) are not composed of conductive material, then there is a possibility to perform sub-surface ultra-high-frequency reflective diagnostics only up to the first layer, made of conductive material.

For multilayer composite materials and the use of the reflection diagnostic method, the effect of the summation of the direct ultra-high frequency signal and its reflection from surfaces with different electromagnetic characteristics should be taken into account. If the reflected and direct signals are dephased by about 90 degrees (due to the distance between the sheets in proportion to about 0.5 of the wavelength of the signal), they will compensate for each other. This effect can be avoided both by selecting the appropriate frequency of radiation for the particular type of composite material and by displacing the transmitter and receiver and providing a definite angle between the transmitted and the received signal.

4. Non-destructive testing of composite materials by holographic subsurface radar

Non-destructive testing - Definition

Non-destructive testing (NDT) is a testing and analysis technique used by industry to evaluate the properties of a material, component, structure or system for characteristic differences or welding defects and discontinuities without causing damage to the original part. ***[8]***

NDT also known as non-destructive examination (NDE), non-destructive inspection (NDI) and non-destructive evaluation (NDE).

Holographic subsurface radars (HSR) are not often used, probably due to the fact that high attenuation of electromagnetic waves will not allow sufficient depth of penetration. It is true that the fundamental physics of HSR prevents the possibility of changing the receiver gain over time (i.e. depth) to adapt to a lost environment (as possible with impulsive subsurface radar (ISR)).

However, the use of HSR to investigate shallow subsurface objects, defects or inhomogeneity is an increasingly proven field of application.

In this case, HSR can record higher resolution images than is possible for ISR images.

Holographic subsurface radar is characterized by the requirement for routine surface scanning to record holograms. In this sense, HSR is an analogue of the optical hologram technology proposed and implemented by D. Gabor in 1948 **[9]**. The method proposed by Gabor can simply be illustrated with an example of recording a hologram in a point object. Axially symmetric hologram of an object point can be recorded on a flat plate such as an interference pattern between a coherent plane wave with constant phase perpendicular to the plate, and the waves that are scattered from a point object. A schematic representation of the Gabor optical hologram method for a point object is shown in fig. 1**[10].**

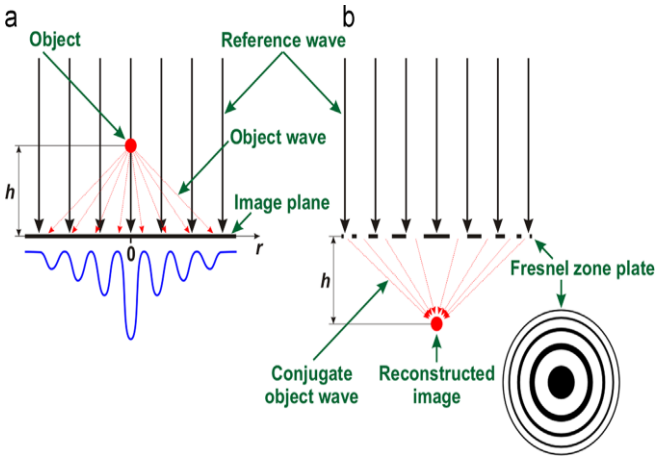

Fig. 1: *Optical hologram recording (a) and reconstruction (b)* ***[10]***

The plate that records the interference pattern of waves is called a hologram. Unlike optical imaging, a microwave hologram could record not only the intensity of the waves scattered by the object, but also information about the phase of these waves. When the optical hologram is illuminated by coherent light of the same wavelength used for recording, a virtual three-dimensional image of the object is projected across the screen. In the case of a point object, the hologram is a Fresnel lens and the projected or reconstructed object is simply the point itself **[9].**

The Gabor method for recording holograms has many drawbacks in terms of the quality of the hologram and the convenience of its application. A new step in the development of holography was made by E.N. Leith and J. Upatnieks after the invention of the laser **[9]**.

A method using a coherent beam of light at an angle to the recording plate is proposed. A diagram of this type of holography is presented in fig. 2. Subsequent innovations in optical holography include the use of various combinations of mirrors and light. Nevertheless, holographic technology is of great use in radar. For example, holographic radars were designed to detect weapons concealed on human bodies at airports.

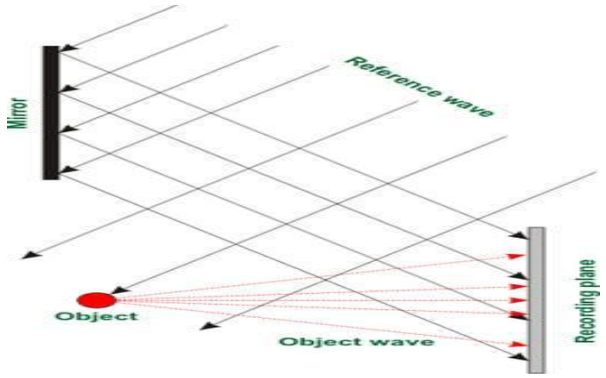

Fig. 2: Optical hologram with inclined light beam **[9]**

Radar holography in the atmosphere or outer space also has many features in common with optical holography, due to the lack or very low level of attenuation and dispersion of electromagnetic waves in these environments.

Holographic subsurface radars are designed to investigate heterogeneous environments with relatively high attenuation rates and sometimes high dispersion. This property can have a great influence on the recording of multifaceted holograms.

All these factors impair the quality of microwave holograms and, in many cases, make the recording of holograms impossible. The theoretical explanations for the influence of the properties of the sources on the quality of the subsurface holograms were discussed recently by N. Chubinski **[11]**. Surface attenuation and surface heterogeneities limit the maximum effective penetration depth for HSR. It is important to emphasize that the ISR has a clear advantage over the HSR in terms of effective penetration depth because of the possibility of applying a variable time gain to a strobe beam for selectively amplifying deeper reflections that have a longer "time-of-flight" (a method of measuring the distance between a sensor and an object based on the time difference between the signal being transmitted and returning to the sensor after being reflected by an object). Since time-of-flight is irrelevant to HSR, the main application of HSR is related to shallow depths.

At shallow depths, where applicable, the main advantage of HSR is the ability to record higher resolution images in the search plane than the ISR. High resolution at shallow depths is crucial for many applications, including the diagnosis of composite materials.

The catastrophic loss of the US space shuttle Columbia has forced researchers to find new possible methods and devices for non-destructive testing and evaluation of the space shuttle's thermal protection system, as well as the insulation foam of an external fuel tank. Such diagnostic methods can be useful not only for current spacecraft, but also for promising spacecraft such as the Orion manned spacecraft **[10]**.

The basic problem with non-destructive testing of space vehicles thermal protection systems is that the task requires examination of a layer of dielectric material, applied directly on the metal support shell. If such composite structures were investigated by means of pulsed subsurface radar, the absorption of a radiated pulse between the metal surface and the radar antenna would significantly complicate the detection of heterogeneities and defects in the dielectric heat-shielding material. Holographic subsurface radars do not contain this disadvantage since the signal reflected by the metal surface parallel to the surface of the radiation shielding material has a constant phase and does not affect the quality of the recorded radar images.

5. Status of research on the problem

New ultra-high-frequency non-destructive testing technologies can be based on the technology used to create so-called holographic subsurface radars, developed at Bauman Moscow State Technical University and found widely application in the diagnosis of building structures.

Preliminary experiments conducted jointly with State Space Corporation ROSCOSMOS and Vikram Sarabhai Space Center, Indian Space Research Organization, Kerala, India on presented specimens of various composite materials containing porous and elastic components, including specimens of thermal insulation coatings for space new generation rocket launchers have shown the promise of this direction.

The analysis of the reports presented at the International Conference on Non-Destructive Control in the Aerospace Industry **[9,10]** shows that the methods of ultra-high frequency diagnostics were presented only in the report of the Bauman Moscow State Technical University **[10]**. It is known that NASA, USA, a few years studies have been conducted on ultra-high frequency diagnosis of insulating coatings of rocket containers, but probably due to the use of other methods of information processing are not achieved good results and these studies have not received development in the US **[10,11]**.

The holographic subsurface radars **[7]** developed at the Bauman Moscow State Technical University have a working frequency range of 1.6 to 6.8 GHz and are commercially available and are used for the diagnosis of building structures both in Russia and in other countries. The authors of the project have received a government award in science and technology for their development. At the same time, it is necessary to continue the studies related to the reflection of electromagnetic waves from the internal structure of the given materials, as well as to carry out a number of studies in order to develop new technologies for ultra-high frequency diagnostics, including in other frequency ranges. Due to the use in the aerospace industry of a number of low-attenuation dielectric coatings, such as fiberglass, polyurethane, quartz, ceramics, non-metallic nanoclusters, etc., one direction in this direction is related to the use of a 24 GHz frequency band leading to quality improvement the image and the possibility of recording minor defects in the components manufactured. To evaluate this possibility, it is necessary to evaluate the specific vibration damping at a frequency of 24 GHz for some composite materials using them.

6. Conclusion

A summary of the theory, technology and applications of holographic subsurface radar is presented in this paper. The main advantages and limitations of commonly used pulse radars are also considered. In many practically important cases the depth of penetration is insufficient and the quality of recorded images does not allow reliable identification of detected objects. However, the proper choice of the type of sounding signal and its frequency range can lead to useful results that cannot be achieved by other non-destructive diagnostic methods. A typical area of application for holographic subsurface radar is the study of opaque shallow-depth objects where high resolution is desired. In these cases, it is possible to define the shape and dimensions of the targets and elementary objects with sufficient accuracy and to formulate reasonable assumptions about their nature for developing image-based classification pictures.

ACKNOWLEDGEMENT

The results of this development have been achieved in accordance with Contract № KP-06-RUSSIA /22 dated September 28, 2019 between IMSTCHA-BAS and the National Science Fund of Bulgaria (NSFB) for the implementation of the Project "New technologies for nondestructive testing of composite materials in aerospace industry", funded by NSFB as a result of the "Bilateral Cooperation Program Competition 2018 - Bulgaria - Russia 2018-2019".

Bibliography:

[1] Yavor Boichev, N. Dyulgerov, "Metalphysical Investigations of Composite Aluminum Alloy with Microcrystalline Structure", "Metal Science, Hydro and Aerodynamics, National Security", 2013, ISSN:1313-8308, p.p. 219-221;

[2] Boychev Y., "Investigation of plasticity of composites based on aluminum alloys with microcrystalline structure at different test temperatures", Proceedings NDT Days' 2014, 2014, ISSN:1310-3946, p.p. 214-216

[3] Yavor Boichev, G. Stefanov, N. Dyulgerov, S. Gyurov. "Structural features of compact composites with a microcrystalline structure based on aluminum alloys", Proceedings - Fifth National Conference with International Participation, " Metal Science, Hydro and Aerodynamics, National Security'2015 ", 2015, ISSN:1313-8308, 200-203

[4] Dyulgerov N., Boychev Ya. Preparation and properties of real-size composites and microcrystalline structure based on aluminum alloy with TiC addition. XXVI International Conference "NDT days '11" Proceedings, 2011, p.p. 234-235

[5] Genov BG, "Possibilities for Using Non-Destructive Control Methods in Ballistic Protection Systems Assessment", International Conference "Non-Destructive Control Days" 2011, Sozopol, 11-14.06 2011, ISSN 1310-3946, p. 107-110 Genov B., The Need for the Implementation of Non-Destructive Control Methods in the Stages of the Lifecycle of Defense Products, International Conference "Days of Non-Destructive Control" 2012, Sozopol,11-14.06 2012, ISSN 1310-3946, стр. 363-365

[6] Borislav G. Genov, "Model for evaluation of the technical state of rocket propulsion engines based on the results of non-destructive testing" International Conference "Days of Non-destructive Control" 2018, Sozopol, June 2018, published in NDT Days, Volume I / Issue 4 (2018), ISSN: 2603-4018 (print), 2603-4646 (online), p.p. 484-493

[7] Borislav G. Genov, "Criteria for Choosing Non-Destructive Control Methods in the Ammunition Lifecycle", International Conference "Days of Non-Destructive Control" 2018, Sozopol, June 2018, published in NDT Days, Volume I / Issue 4 (2018), ISSN: 2603-4018 (print), 2603-4646 (online), p.p. 494-503;

[8] https://www.twi-global.com/technical-knowledge/faqs/what-is-non-destructive-testing;

[9] Sergey I. Ivashov, Vladimir V. Razevig, Igor A. Vasiliev, Andrey V. Zhuravlev, Timothy D. Bechtel, Lorenzo Capineri, "Holographic subsurface radar: TECHNOLOGY AND APPLICATION", JOURNAL OF RADIO ELECTRONICS, N 10, 2010, electronic journal, ISSN 1684-1719;

[10] S. Ivashov, V.Razevig, I.Vasiliev, T.Bechtel, L.Capineri, „Holographic subsurface radar for diagnostics of cryogenic fuel tank thermal insulation of spacevehicles", NDT&E International 69 (2015), pp. 48–54, ISSN: 0963-8695;

[11] N. P. Chubinsky, "Possibilities of holographic methods at sounding of lossy media", Proceedings of 4th Russian conference RadioPhysics Methods in Remote Sensing, Murom, 30 June – 3 July 2009, pp. 47-60,(in Russian).

Available: http://www.mivlgu.ru/conf/murom2009/img/doclad/lecture/3.pdf.

Size and speed of data generated by Fleet Management Software

Nikolay Kaskatiiski.
University of National and World Economy Sofia, Bulgaria
nkaskatiiski@dxc.com

Abstract: *The paper looks at the relation between the number of transport domains (cars, trucks, buses, ship, etc.) and the size of data, generated in fleet management software. Nowadays, such software is stored and run on a cloud and users do not need to care about the size limitation, just for the price. If using a solution on premises, the cost includes creating and supporting infrastructure and licences. Software developers should care for the scalability of the application time and also managing bottlenecks, that are likely to appear in data flow due to the size of the management program.*
Keywords*: CLOUD, ON PREMISES, FLEET MANAGMENT, AUTOMOTIVE,* SAE J1939

1. Introduction

In present life, goods are manufactured all over the globe and are transported to customers in their respective countries. Internet trade increases the demand for fast and reliable end-to-end transportation of goods. Within a company, the task of efficiently managing the utilization of different transportation means is delegated to a fleet management system (FMS). This is software, used in enterprises, responsible for acquiring, maintaining, planning and generating profit, related to transportation company actives. Such software is part of company's tools, used to maximize profit and reduce cost. FMS tool tracks all available transportation means and classifies them depending on type and usage. It assigns to the elements of the fleet various parameters depending from business needs. Planning maintenance with cost and time, predicting supplies and spare parts are part of the requirements to the system.

2. Structure of Software for Fleet Management

Fleet management software might consist of several logical parts - Figure 1. These are telematic system, service provider, and central authority system (order & fleet management).

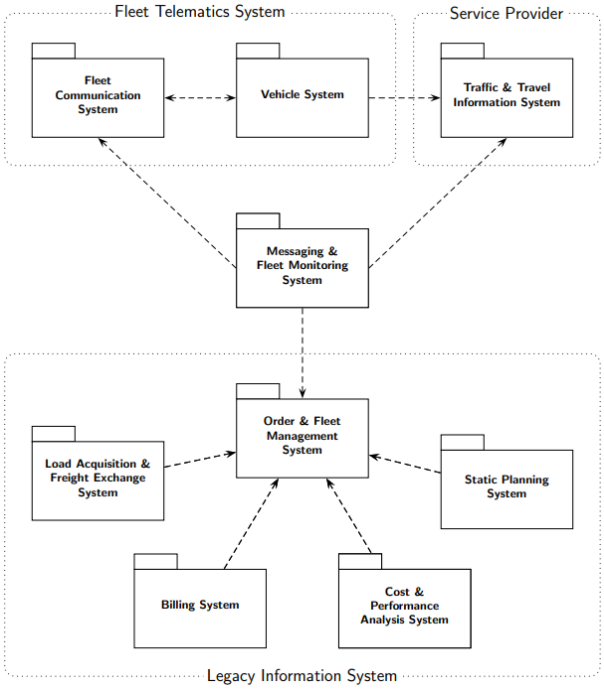

Figure 1. *Block model of Software for fleet management.*

The *telematic system* is the part, responsible for collecting data. It is placed on the vehicle and is unique for each item in the fleet. Its main requirements are to inform driver for changes in the environment and to transmit data to the information storage.

The *service provider* is responsible to feed fleet management system with information that is needed to work properly but is not part of telematic system. Data provided by this system might be relatively static as geo data or dynamic as weather conditions or traffic conditions

The *order & fleet management* is the "brain" of the system. Data received from telematic system and service provider is stored and processed in this unit of FMS. This is the unit, where transportation requests are made, reports for different needs are generated and visualized. Users interact with FMS trough this part of the package to post requests related to management of transportation means. Based on algorithms, defined in this logical unit, dispatchers can generate messages and interact with drives trough telematic system. Order & fleet management system is typically interacting with other systems in the enterprise like ERP, cost and performance analysis, planning systems, etc. [1].

3. Strategy for software hosting

Every enterprise has its own strategy and dedicated teams to manage software infrastructure, with common goals - reduce cost and increase efficiency. When integrating a new package in the corporate software environment a decision must be whether this software will run on premises, or be hosted on a cloud. In the past, each organization has its own hardware infrastructure and dedicated teams to manage their software products and such solutions are called *on premises*. Nowadays there are data centers, where an organization can outsource the software management - clouds. There are some features for both approaches that must be considered, when a strategy for a new software is drawn. The key difference between the two approaches is who is responsible for what and who is responsible for the risks. Cloud-based solutions require the organizations to pay a subscription fee to the provider, in order to use the software. The software is usually accessed online through a server owned by the software provider.

Under cloud solutions, the software vendor is responsible for the server infrastructure data integrity, updates, backups, and security measures. Still company must have wideband and reliable internet connection trough data canter of the software provider. Organization relies on service level agreements (SLA) and ability of software provider to manage a possible crisis, related to system malfunctioning. Updates of software are regularly received, liked or not. It is not possible to have dedicated features and customizations, common to all users of a package.

On-premise software requires the organization to pay the cost of the software, upfront. In exchange, they receive a product with full licensing, capable of being used on the company's server. Organizations are thus required to manage and maintain their physical computer servers internally, primarily when backups and upgrades are being performed. As data is stored in house all concerns about management and security are internal for the organization. It is possible software owner to provide custom feature or allow organization to build them self as organization has a higher degree of control when implementing the system [2].

During operation time of the package, there is certain cost for transferring data from telematic system to order management past of the system. The amount of this data depends of now much information system is logging form one unit, how often this information is collected and how many unites are managed by the fleet management system.

4. Data Generated by Transportation Means

Data from the vehicle reaches the data storage system, after passing through several levels. First is the physical - transformed into electrical signal. Physical data values are temperature, speed, humidity, fluid level, pressure, etc. At the second stage - the electrical signal is digitally coded, so that can be processed further. Then data must be transmitted from the mobile unit to the stationary ground network. From there it is the network, that transfers data to the storage and also for processing by the fleet management system.

There is various of environmental parameters that must be monitored to assure smoot and effective work of a vehicle. Some are related to engine itself, that allows them to operate and to monitor if it is in working conditions. Others are monitoring for hazardous situation and provide feedback to manage such situations. Such data is handled and managed by the systems of the vehicle. In respect to fleet management, this information is not so valuable unless it leads to conditions, where the vehicle is not operating normally. Other types of environmental parameters that do not have direct impact of transportation means but are valuable for the fleet management system are the position of the vehicles, its speed, and its destination. On top of them, the fleet management system must be interested by the driver who is operating the unit, the cargo's conditions if applicable for the unit, energy stored in the vehicle (level of gas tank or battery charge) and currently consumed energy. In modern system all this data is collected and proceeded by Electronic Control Unit ECU. To reduce cost and make some components interchangeable, as well to ease the maintenance of the transportation means, manufacturers follow data exchange standards. Data between sensors and ECU could be analog signal or digital. The most popular standard is Controller Area Network (CAN bus) [3]. This is a robust vehicle bus standard designed to allow microcontrollers and devices to communicate with each other's applications without a host computer. It is a message-based protocol, designed originally for multiplex electrical wiring within automobiles to save on copper, but can also be used in many other contexts. For each device, the data in a frame is transmitted sequentially but in such a way that if more than one device transmits at the same time the highest priority device can continue while the others back off. Frames are received by all devices, including by the transmitting device. As the CAN standard does not include tasks of application layer protocols, such as flow control, device addressing, and transportation of data blocks larger than one message, and above all, application data, many implementations of higher layer protocols were created. Several are standardized for a business area, although all can be extended by each manufacturer. Among these implementations are SAE J1939 in-vehicle network for buses and trucks and SAE J2284 respectively for passenger cars [4].

SAE J1939 is a high-level communications protocol, which operates on a CAN bus. SAE J1939 specifies exactly how information (e.g. engine RPM) is exchanged between electronic control units (ECUs) on a vehicle. Information is exchanged in data frames consists of header or datalink, actual data or message and several control bits. Datalink is encoded into the 29-bit CAN identifier and contains bites for: Priority, Extended Data Page, Data Page, Protocol Format, Protocol Specific, and Source Address - Figure 2.

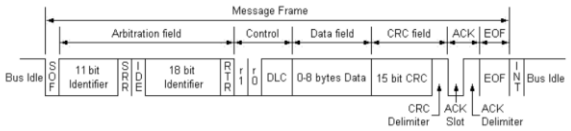

Figure 2. *Data frame in SAE J1939.*

A message is in one or more CAN data frame and contains information exchanged between devices on the datalink. J1939 has three different allowed message sizes, they are: 3 bytes, 8 bytes, and variable length. Most messages in J1939 are 8 bytes in length. This allows for a more efficient use of the network bandwidth by maximizing the amount of data on the network by reducing the number of messages. Variable length messages are messages with a length from 9 to 1,785 bytes. These messages are too large to fit in a single CAN data frame and must be fragmented by the transmitter and reassembled by the receiver. This process is defined by J1939's transport protocol which is specified by J1939-21. The size of one data frame all together is estimated at 16 bytes.

5. Data Exchanged Between Mobile Unit and Stationary Systems

Following registration of environmental parameters and conversion into electrical signals is to send the information form vehicle to stationary network and fleet management system. Nowadays under stationary network is understandable Internet, assuming FMS is connected to internet. Data exchange could be done online or offline. Offline is when data is stored in memory of the unit and then uploaded to internet on occasionally on time basis. Examples when vehicle is stationary at depot connected to local network via Bluetooth, Wi-Fi, etc. or information is transferred from device memory card. Online transmission is continuous process of transferring information for status of the unit. Most widely used mediums is cellular or satellite network. In addition, other means of exchange data dedicated to transportation exists such as TETRA (TErrestrial Trunked Radio) a European standard for modern digital trunked radio. For civil systems in Europe the frequency bands 385-390 MHz, 395- 399.9 MHz, 410-430 MHz, 450-470 MHz, 870-876 MHz, and 915-921 MHz, have been allocated for TETRA by ERC Decision (96)043. Data transfer with TETRA is at 7.2 kbps. Dedicated Short Range Communication Dedicated Short Range Communications (DSRC) is a short to medium range wireless communication technique specifically designed for automotive use, i.e. vehicle-to-vehicle and vehicle-to-infrastructure communication. Due to the short range of the signals, DSRC is useful to provide location-based services. Today, the main application of DSRC is Electronic Toll Collection (ETC). DSRC systems use infrared or the radio spectrum, particularly microwaves in the frequency bands 5.795-5.805 GHz and 5.805-5.815 GHz [5].

6. Use Case, Results and Discussion

To do some calculation, we assume that an organization manages a fleet of 50 unites (the number is chosen to be relatively small compare to fleet of rental vehicles and could be used as base for future calculation in relation to number of unites) and is concerned to have information for each unit at real time and reasonable price. To reduce the data exchanged between telematic system and central authority system of FMS, some data will be transmitted less frequently from the other and some conditions will be present to send data or not. For FMS resolution of 1 sec is considered as acceptable for time critical events. Resolution of 10 secs will be used for dynamic events and 60 sec for non-critical parameters.

Table 1: *Values that will be transferred for unit to FMS. Note that some J1939 messages (PGN) contains more than one value of interest.*

Critical values	Dynamic values	Non-critical parameters
• Engine Seed • Engine Torque Mode • Driver's Demand Engine-%Torque See PGN61444	• Fuel Level See PGN65276	• Miles Driven • Axle weight (kg) See PGN65217
• Engine Oil Pressure • Engine Oil Level • Engine Coolant Level See PGN65263	• Engine Coolant Temp • Engine Fuel Temp • Engine Oil Temp See PGN65262	• Engine Hours • High-resolution vehicle distance • Service distance • Tachograph information See PGN65253
• Brake switch (on/off) • Clutch switch (on/off) • Cruise control (on/off) See PGN65132	• Vehicle Position See PGN65267	• Temperature in cabin • Temperature in cargo bay • Humidity in cabin • Humidity in cargo bay See PGN652XX
	• Time/Date See PGN65254	
	• Compass Bearing • Navigation-Based Vehicle Speed • Pitch • Altitude See PGN65256	

According to data in Table 1, there are 3x60+5x10+3 = 266 messages per minute or 3.88 per second. As it is stated earlier, one message is 16 byes and if vehicle identification number (VIN) is used to identify the unit from where message is coming with size of 17bytes, thus the size of the message transmitted is 33 bytes. The amount of data generated by the unit for one second of active logging will be 128 bytes, for one hour 450 kB. Assuming average of 9 hours operation per day and 22 days in month data transmitted per month is calculated at 87Mb and if operating 24/7 the amount will be 316Mb. Thus, for fleet of 50 unites we have around 4.2 to 15 GB per month data transfer from vehicles to servers.

For pricing of Amazon S3 storage is counted as well as the requests for PUT, COPY, POST, LIST, GET, SELECT. If each unit is collecting and uploading data every 10 sec a compromise between real time and price for upload, then a unit working 9 hours for 22 days is generating 71 280 server requests or if 24/7 requests are 259 200. And for fleet of 50 vehicles between 3,5 and 13 million

According AWS calculator for S3 [6] to upload store and download data for a fleet of 50 units running 24/7 :

- Tiered price for: 15 GB
- 15 GB x 0.0245000000 USD = 0.37 USD
- Total tier cost = 0.37 USD (S3 Standard storage cost)
- 13,000,000 PUT requests for S3 Storage x 0.0000054 USD per request = 70.20 USD (S3 Standard PUT requests cost)
- 15,000 GET requests in a month x 0.00000043 USD per request = 0.0065 USD (S3 Standard GET requests cost)
- 15 GB x 0.0008 USD = 0.012 USD (S3 select returned cost)
- 15 GB x 0.00225 USD = 0.0338 USD (S3 select scanned cost)
- 0.3675 USD + 0.0065 USD + 70.20 USD + 0.012 USD + 0.0338 USD = 70.62 USD (Total S3 Standard Storage, data requests, S3 select cost)
- **S3 Standard cost (monthly): 70.62 USD**

Next, let's make some computation on the resources in the cloud. Basic FMS must monitor for errors and potentially hazardous situations as much as close to real time. Assuming every 10 secs and those checks will take no longer than 100ms. This is part of automation of the system that monitors each unit in real time and reports/take actions according programming logic.

On the other hand, we have users interacting with the program giving new orders new destinations, generating reports working with collected data. Those are relatively big request compare to the one that are monitoring units. Users will do large request lasting 10 secs every 10 minutes, as there will be 10 users connected during working hours. These are average assumptions. On a monthly basis 269760 request with average length of 961ms and 2GB of memory:

- RoundUp (900) = 900 Duration rounded to nearest 100 ms
- 269,760 requests x 900 ms x 0.001 ms to sec conversion factor = 242,784.00 total compute (seconds)
- 2 GB x 242,784.00 seconds = 485,568.00 total compute (GB-s)
- 485,568.00 GB-s - 400000 free tier GB-s = 85,568.00 GB-s
- Max (85568.00 GB-s, 0) = 85,568.00 total billable GB-s
- 85,568.00 GB-s x 0.0000166667 USD = 1.43 USD (monthly compute charges)
- 269,760 requests - 1000000 free tier requests = -730,240 monthly billable requests
- Max (-730240 monthly billable requests, 0) = 0.00 total monthly billable requests
- Lambda costs - With Free Tier (monthly): 1.43 USD
- Time for which Provisioned Concurrency is enabled: 8 hours = 28800 seconds

Pricing calculations

- 10 concurrency x 28,800 seconds x 2 GB x 0.0000050147 USD = 2.89 USD (Provisioned Concurrency charges)
- RoundUp (10000) = 10000 Duration rounded to nearest 100ms
- 10,000 requests x 10,000 ms x 0.001 ms to sec conversion factor = 100,000.00 total compute (seconds)
- 2 GB x 100,000.00 seconds = 200,000.00 total compute (GB-s)
- 200,000.00 GB-s x 0.0000117011 USD = 2.34 USD (monthly compute charges)
- 10,000 requests x 0.0000002 USD = 0.00 USD (monthly request charges)
- 2.89 USD + 2.34 USD + 0.00 USD = 5.23 USD
- **Lambda costs for Provisioned Concurrency (monthly): 5.23 USD**

Estimated cost of data storage and manipulation on the cloud is shown in Figure 3.

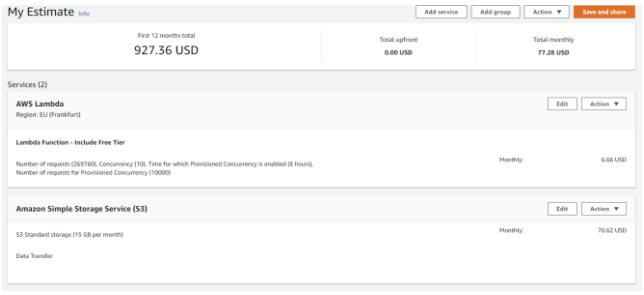

Figure 3. *Estimated price for data storage and data processing in AWS.*

7. Conclusions

It must be found a balance between requirement to have data in real time and the quantity of data transferred between telematic system and stationary part of FMS. Data generated by vehicle is continuous (analogue). For the size of the data transferred between mobile units and stationary system is important to select the frequency of reported data based on priority and based on events that are detected on the unit itself. Calculation for the size of data done for one vehicle are proportionally to number of unites present in the system from one type. In case of variety of unit types, they must be classified and calculation to be done depending of vehicle class. As the size of the data increases with number of units this could be a key factor to go on cloud or stay on premises.

Larger enterprises can invest significant capital in on-premise FMS solutions, but smaller – can't. For medium and small businesses have limitations on their budget, so cloud FMS software alternatives are the only answer. They simply save time and money.

Whichever the case, every successful business requires a healthy and dynamic data ecosystem. Having a reliable and scalable infrastructure in place which can support end-to-end visibility of data flows, fast and secure file transfers, data transformation, and storage is integral to success.

8. References

1.Goel, Asvin, *Fleet Telematics*, Zaragoza, Springer, 2008, ISBN: 978-0-387-75104-7, page 86
2.Fisher, Cameron, A. J. I. B. M., **2018, 8,** ISSN Online: 2164-5175 pages 1991-2006, (2018)
3.*SAE J1939* , https://en.wikipedia.org/wiki/SAE_J1939
4.Simma Software, Inc, *J1939*, http://www.simmasoftware.com/j1939.html
5.Moradi-Pari, Ehsan, *5.9 GHz Spectrum Sharing*, Springer, Nature Switzerland AG 2019 R. Miucic (ed.), Connected Vehicles, Wireless Networks ISBN 978-3-319-94784-6, page 203
6. 2020, Amazon Web Services, Inc., AWS Pricing Calculator, https://calculator.aws/#/estimate

Analysis of the causes that generate traffic accidents

Angela Popusoi
Faculty Constructions and Installations „Gheorghe Asachi" Tehnical University of Iasi
angela374@mail.ru

***Abstract**: The article describes the causes of serious road accidents, as well as the analysis of the influence of the environment on the safety in circulation. In addition, the road network schemes are subject to analysis, ie to what extent they influence the safety of the road. The geometric elements of the road, the layout, the curves in profile. The route of a road has to provide good guidance through its geometry in space and through the elements in the environment and the longitudinal profile, transversal profile, intersections, visibility analysis during the driving process of a vehicle. Influence of road function on traffic safety. For developed countries, the road network is defined on the basis of the road classification in terms of the function it performs, with a focus on the ability to collect or transit traffic. Influence of road equipment on traffic safety. Influence of running surface characteristics on traffic safety. The ruggedness, flatness and waterproofness of the road surface are absolutely indispensable, ensuring the comfort and safety of the traffic. The influence of the human factor on the safety in circulation. Traffic participant is the first link in the road safety chain. Whatever the technical measures adopted, the effectiveness of road safety policy ultimately depends on the behavior of the traffic participants. Violation of pedestrian traffic rules. The circulation of the means of transport is accompanied by energy waste, in the form of noise and vibration, which also has an influence. The forecasts for the development of the transport network show that the sudden increase in the number of transport units increases the risk of an increase in the number of accidents. The vehicle, its influence on the safety in circulation. According to the data on the distribution of accidents by types of vehicles, we can see that the group with the highest number of accidents is that of cars. Conclusions and recommendations are outlined.*
***KEYORDS**: ACCIDENT RUTIER, PIETON, REȚIEUA STRADALĂ, INTENSITATEA TRAFICULUI, DRUMURI*

1. Introduction

Road transport is an integral part of our lives. Whether we are driving a car, a motorcycle or a bicycle, are in a public transport or just pedestrians, we are all participants in traffic. Every day, we spend considerable time moving from one place to another. Crowding, traffic jams, blocked intersections, aggression, young rebels behind the wheel, careless pedestrians, noise pollution, illegally parked cars, all define contemporary traffic where no one seems to follow the rules. Unfortunately, all these problems translate in the very large number of road accidents. Of all transportation accidents, road accidents cause the most casualties each year.

2. The causes that generate road accidents

The influence of the road environment on traffic safety. The Road Environment - Man - Vehicle system is the conceptual framework in which road traffic, with all its components, must be understood and analyzed.

The totality of streets and spaces reserved for the pedestrian and vehicular traffic of a city constitutes the traffic network or the street network; the elements consist of bars (streets) and nodes (intersections, squares, centroid, etc.), to which are added the extended parking arrangements (parking lots, garages).

A very important index in establishing traffic networks is the percentage of land use of the total area of the traffic network in the entire area of the city. Statistically, such occupancy rates vary between 10% and over 40% of the city. Experience has shown that the ground occupancy of traffic networks of values close to 20% is reflected with satisfactory results in traffic, but this indicator also depends on the size of the city and some local conditions.

The different plan configurations of the traffic networks, in particular of the main road network, distinguish several types with common characteristics. Differentiations between types occur depending on the multitude of conditions that have influenced the structure of existing cities since the origins of their formation. Thus, sets of different types of street networks can be found in the same city, developed in different eras.

Regardless of the causes that generated them, there are two main categories of network types: geometric more or less rigid, and free.

From the point of view of traffic, each of these networks has positive and negative characteristics, so the inclusion in one of these types must result from comparative analyzes.

In general, for the development of modern traffic, the aim is to achieve clear networks of interzonal and external connections, as direct as possible and without embarrassing interference. Of course, the elements of the traffic network cannot and should not be identified with the traffic vectors of the zonal distribution, but they must satisfy them in the best conditions, in this sense, the configuration of the network, as a type, is not necessarily an essential condition. , but it must still be taken into account which of the types would be most appropriate for local conditions and coordination with the provisions of the systematization of land use and traffic distribution, in the current and future traffic conditions.

The geometric elements characteristic of roads represent the totality of the component elements of a road in situation plan, longitudinal profile and transversal profile.

Studies conducted over time on road accidents by Kang.J. [1] highlighted a number of connections between the risk of their occurrence and the geometric elements of roads, drawing the following conclusions: the proportion of accidents is 1.5 to 4 times higher in curves than in alignment.

A number of authors have identified some of the risk factors in their studies. For example, they studied the perception of the credibility of the speed limit imposed in relation to certain characteristics of the road according to which the objective risk varies:

- curve: yes / no;
- road width: average / wider than average;
- viewing distance: less than average / average / higher than average;
- opening the scene (presence of objects that block the view);
- left / right vision;
- the presence of the bicycle lane;
- presence of traffic lights;
- trees left / right;
- vegetation on the left / right;
- traffic in the same direction / in the opposite direction [2].

The arrangement of many intersections is the apparent result of evolution over time.

By arranging the intersections, the aim is to allow the crossing of flows and changes of direction and direction, which are necessary to travel a route, minimizing the dangers of accidents and ensuring the best possible flow of traffic, with average speeds and flows, as close as possible to the design speeds and traffic capacities of the component streets of the route.

During the process of driving a vehicle, approximately 95% of the information that reaches the driver is perceived visually. The visual detection process is the only one in tracking the road, as well as the detection of obstacles and the interpretation of road

signs, light signals, markings or other signaling modes. Drivers do not have the ability to observe the road continuously. They blink, notice objects on the other side of the road, look in the rearview mirrors, read the car's appliances, and talk to passengers in addition to other tasks. The process is therefore one of sampling [3].

In the case of developed countries, the road network is largely defined on the basis of the classification of roads in terms of the function they perform, with an emphasis on the ability to collect or transit traffic.

Traffic planning and infrastructure design have a particular impact on road safety, reflected for example both in the appearance of streets in residential areas for accidents involving pedestrians and in the case of an urban traffic network with a large number of intersections, which poses a danger, high accident due to the lack of separation of traffic of all categories of road users.

The correct location of traffic signs makes a considerable contribution to improving the safety and efficiency of the transmission network. They must be designed to convey clear and unambiguous messages to road users so that they can be understood quickly and easily. In developed economies, road signs comply with the regulations and standards in force to ensure their consistency across the country.

The quality of the road surface essentially influences the traffic conditions. The safe operation of the road is influenced by the way the road tire contact is made. The lack of permanent contact of the tires with the road reduces the possibilities of maneuvering and braking and can generate undesirable road events.

The roughness, flatness and impermeability of the road surface are absolutely indispensable, ensuring the comfort and safety of traffic.

Pits, veils, sills, sanded surfaces, damaged edges and poor sidewalks are just some of the factors involved in losing control of the vehicle and skidding.

There are no statistics on accidents caused by potholes, but it is believed to be the major cause of accidents that occur at high speeds, especially for two-wheeled vehicles. The pits are risky, on the one hand on impact, on the other hand when trying to avoid them.

Roughness. Roughness is the property of the road surface to show roughness. This ensures the stability of the vehicles in motion, by achieving the best possible grip between the tire and the track.

Flatness. Flatness is a characteristic of the track and represents the its uniformity. Its quality can be affected by different types of cracks, deformations or disintegration problems.

Defects related to the flatness of the road surface directly influence the comfort level of the occupants of a vehicle, the cost of operating the road and can also have adverse effects on road safety.

Impermeability. Waterproofing is a qualitative parameter of the running surface and has a special importance on the behavior of the road structure in operation.

If the wear layer of the roadway does not ensure the impermeability of the road, water from rain or melting snow enters by infiltration into the layers of the road structure. In this situation, there are a number of deficiencies in each road layer, which is influenced by the presence of water in its material structure.

The traffic participant is the first link in the road safety chain. Whatever technical measures are taken, the effectiveness of road safety policy ultimately depends on the behavior of the traffic participant.

Worldwide, the human factor is responsible for 80-90% of road accidents. Starting from the premise that people are prone to commit various types of errors and that the human factor has a very important role in accidents, since the '80s, more and more efforts have been made to research and understand these factors.

Below is a list of the most common causes of fatal road accidents:

1. Inattention and daydreaming at the wheel - 62%
2. Use of mobile phone -12%
3. Interest in an event, object, person from outside - 7%
4. Conversations with other occupants in traffic - 5%
5. Using or searching for an object in the car - 2%
6. Eating and drinking - 2%
7. Setting the volume and air conditioning - 2%
8. Use of other systems adjacent to the machine: adjustment of side mirrors or seats - 1%
9. The movement of a pet or an insect in the habitat -1%
10. Smoking -1% [4].

All these are the basis for the formation of the most common causes of road accidents: excessive speed, failure to give priority, violation of pedestrian traffic rules, driving drunk vehicles.

In the hierarchy of causes of accidents with serious consequences, the second place in terms of frequency is not given priority. It has been observed that these accidents are mainly grouped in the area of intersections, as a result of:

- the inattention of the drivers when crossing the space for reading the regulatory indicators;
- failure to take into account the influence of meteorological factors on visibility and the optimal stopping distance;
- incorrect assessment of the speed and distance of vehicles on the priority road;
- incorrect assessment of the distance from the vehicle, which comes from the opposite direction caused by the rear uninsurance.

Research has shown that noise influences aggression, because it amplifies the intensity of the state that has already been caused:

- to some extent this can be seen as a result of the direct influence of noise on frustration. The connection between the noise level and the degree of aggression seems to be given by the level of control that the subject has over the noise. If the individual has no control over the duration or volume of an irritating noise, the level of aggression increases;
- noise also tends to cause stress and makes concentration much more difficult. The horn is so overused in traffic that it becomes almost more important than the brake or steering wheel of a car.

The car crowds pedestrians on sidewalks that are permanently reduced in area, reducing the possibility of socialization and perception of the urban environment. Thus, in modern cities, the car that was conceived as a fast means of movement violates the freedom and possibility of safe movement of pedestrians, especially in city centers.

According to the data on the distribution of accidents by vehicle type, we can see that the group with the highest number of accidents is that of cars. In conclusion, road safety measures to reduce accidents will apply mainly to, but not limited to, this category.

3. Studies conducted on Stefan cel Mare Street in the city of Chisinau Republic

The traffic intensity was analyzed on Stefan cel Mare Street in Chisinau, Republic of Moldova, depending on the time of day. We build a graph of the difference in traffic intensity during the day.

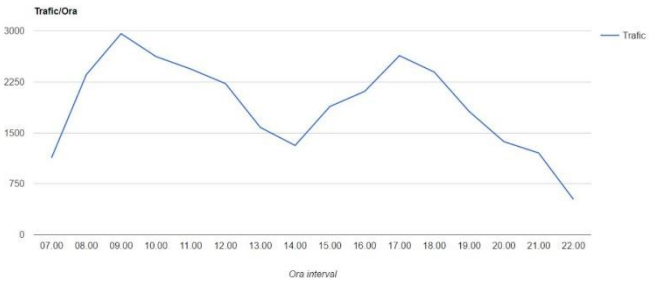

Fig.1 *Variation of traffic intensity during the day.*

Analyzing road accidents according to the time of day, we build another graph. [5]

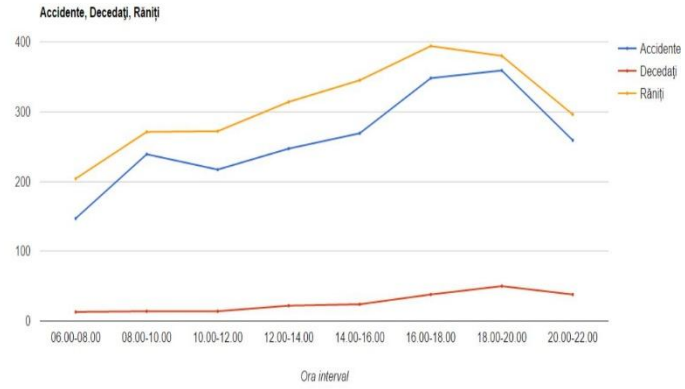

***Fig.2** The difference of road accidents during the day.*

We make an analysis of these two graphs, we see that the intensity of traffic increases between 08:00-09:00 and 16:00-18:00, and the frequency of road accidents also increases between 08:00-09:00 and 16:00-18:00 which proves that it is a dependence of the frequency of road accidents on the intensity of traffic. The influence of noise pollution on Ștefan cel Mare și Sfânt Boulevard on the frequency of road accidents was established.

The measurements were performed with the sound level meter DT8852 on Ștefan cel Mare și Sfânt Boulevard on 13.04.2016, starting with 12:43 on Libertății Square and until 14:25 on Dimitrie Cantemir Square. The sound level meter DT8852 has been set to determine the level of continuous sound pressure weighted A on the edge of the roadway at a height of 1.2 m. From the curb upwards, setting the maximum sound level (L_max) on the streets:

1. Ciuflea (L_max) = 89.5 dB.
2. Ismail (L_max) = 91.0 dB.
3. Tighina (L_max) = 87.2 dB.
4. Armenească (L_max) = 88.9 dB
5. V.Alecsandri (L_max) = 87.4 dB
6. A. Pushkin (L_max) = 87.0 dB
7. Bănulescu Bodoni (L_max) = 94.0 dB, it is raining
8. D. Cantemir Square (L_max) = 91.2 dB, it is raining

In the measurement process, the maximum sound level was (L_max) = 99.0 dB, when the alarm was on. The values of the noise indicators (L_max), presented above can be represented graphically for each point where the measurements were made.

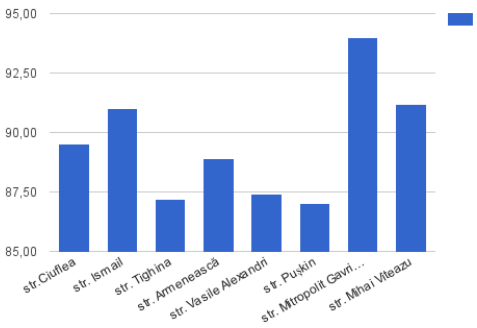

***Fig. 3.** The sound level at the intersections on Ștefan cel Mare și Sfânt Boulevard.*

Why is there a difference in sound level at different intersections? A study was made of the traffic intensity on all the intersections on Ștefan cel Mare și Sfânt Boulevard. Difference in traffic intensity at intersections. We compare these values and see that the noise intensity is higher at intersections where the traffic intensity is higher. So the size of the noise depends on the traffic. It was noticed that the biggest noise is the old trolleybuses and old buses.

From the graph shown in Figs. 3 results that on Ștefan cel Mare și Sfânt Boulevard, the admissible limits of the sound level during the day are: exceeded by 26dB, reason for which measures must be taken to reduce noise pollution.

4. Conclusions

Considering the increase, in recent years, of the degree of self-motorization, changes in the structure of public transport, increase of intercity commuting, it becomes clear that the existing road network (with insufficient technical parameters and traffic capacities) can no longer meet modern requirements. The situation is also complicated by the lack of alternative possibilities regarding the orientation of road connections, which causes the appearance in the central area of intra-urban transit flows in a volume of 50%. At the same time, the city center acts as a node in the structure of public transport, being the most important point of arrival and departure of passengers. It can be concluded that the main streets of the central area, destined for the connection with other urban territories, do not honor their tasks and need reconstruction with the conformity of the technical parameters to the normative ones.

In order to reduce noise pollution and to streamline road traffic on the traffic artery where the measurements were made, provision should be made for:

- introduction of new means of public transport;
- parallel use of green barriers and those built of special materials, noise screens;
- a less noisy road.

Through the consequences for the individual and the society, the analysis of the causes generating road accidents and especially the identification of the directions of action for the prevention of road accidents requires fundamental and experimental researches, to the development of which this work contributes. The situation of road accidents in Moldova, presented in this paper, emphasizes that research is needed to identify measures to improve road safety.

Bibliography

1. Kang, J., Urban Sound Environment, Taylor and Francis Group, London and New York, 2007, p.305
2. Goldenbeld, C & van Schlagen, I. (2007), ,,The credibility of speed limits on 80 km/h rural roads : The effects pf road and person(ality) characteristics'', Accident Analysis and Prevention, 39, p.1121-1130.
3. Burlacu F. A.: Analiza parametrilor de influență a caracteristicilor geometrice ale drumului asupra siguranței circulației rutiere, Raport de cercetare nr.1, București, 2012.
4. http://www.promotor.ro/masini-noi/news/top-10-care-sunt-cele-mai-frecvente-cauze-a…03.06.2015;14784 (Vizitat 8. 04. 2013).
5. http://www.statistica.md/

Geometric parameters in railroad crossing based reconstruction of Iliantsi-Curilo and Curilo-Rebrovo

Vladimir Popov
University of architecture, civil engineering and geodesy, Sofia, Bulgaria
vpopov.fte@gmail.com

Abstract: *Railroad crossings are a point of conflict between rail and road transport. Failure to abide by the rules and their malfunctioning leads to human casualties. The solution is to improve transport infrastructure. In the course of renewal of the railways in the form of rehabilitation, reconstruction, emergency repairs, new construction and more, it is inevitably necessary to intersect road infrastructure. This is done by crossing at one or two levels. During the construction of the main railway lines in Bulgaria, the safety requirements, the load of the road infrastructure, the current speeds, the financial possibilities and other factors led to the construction of many railroad crossings 757 [1]. They are on the secondary and major railway lines, especially outside the large settlements.*
Of course, with the construction of new routes, intersections at two levels are envisaged and constructed [2, 3], but at the same time the railroad crossings on the rest of the railway network requiring higher safety criteria have to be maintained. This necessitates the replacement of many elements of the railway and the pavement [4], which in turn leads to a change in the conditions for the reconstruction of the railroad crossings. The report examines a specific case of construction practice - reconstruction of railroad crossings along the second railway line in the area of Iskar Gorge [5], but the conclusions it requires are valid for most existing railroad crossings.
Keywords*: DESIGN OF RAILWAY LINES, RAILROAD CROSSING, INTEROPERABILITY OF EU RAILWAYS*

1. Introduction

There are 757 pcs in the network of the National railway infrastructure company [1]. Railway infrastructure reviews shows, of which 677 are protected and fully secured. There have changed the EU average by this indicator - we have 17.5% for Bulgaria, against 47% for Germany, 49% for Hungary and 53% for Slovakia. Of these with automatic electrical or manual barriers are related: Bulgaria - 49%, Germany - 46%, Hungary - 20%, Slovakia - 28%, with alarms: Bulgaria - 34%, Germany - 7%, Hungary - 31%, Slovakia - 19%. In fact, they indicate that NRIC is the EU's leader in security screening and that this should be Bulgaria second after Slovakia, with the most incidents of railway crossings.

The long-standing lack of investment in railway transport has led to strong depreciation and inactivity of the elements that must be linked to the need for manufacturers of safety workshops to operate on it and the precision of road infrastructure. They deal with the general case with a dramatic improvement in speed and, in the rare case, with traffic (mostly represented by social and strategic forces along the railway lines). In this part of the budgets, it is recommended to find emergency repairs for the purposes of: maintaining the speed of movement, seeking safety and the continuous availability of information on certain documents and interoperability with the European railway network.

The most common railroad crossing violations are related to the passage of road vehicles at lowered barriers or regularly triggered signage indicating a train approaching, as well as breaking or striking barrier beams [5, 6]. Every incident of a railroad crossing, with the exception of material damage and inconvenience - broken barriers, damaged signaling devices, slowing down or blocking the movement of trains or delays in the timetable for trains running, carries a risk to the life and health of the offenders.

2. Problems and solutions

The reconstruction of external lines outside the scope of European programs is drawned on the basis of a quantitative inventory database by review of expert evaluation, without making a design project [7]. This is leads to many changes in the construction process, which may change the quantities offered.

For reconstruction it is supposed:

- Mix the existing, wooden pavement on the railroad crossing with the new rubber [4];
- Change the construction of rail track with new ballast, CT6 sleepers, type 60E1 rails;
- To reconstruction the rails track along the axis and level to maintain the design speed.

Following the development of design projects, the following difficulties are encountered in the construction process:

- Due to the replacement of the rail track of wooden sleepers or reinforce concrete sleepers ST4 with rails 49E1 with reinforce concrete ST6 sleepers with rails 60E1 is obtained lift leveling with 7-8 cm Figure 1.

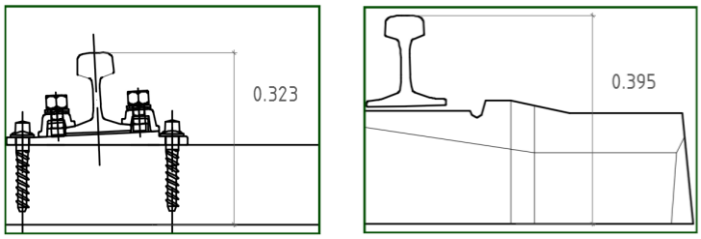

Fig. 1 *Rail track fastening ПАК 68И and SKL14*

- Changing the level of the railway requires a change in the level of road approaches to the crossing.

3. Problems with the height of the railway track

The level of the railway at existing railway lines is determined by the level of the solid points in the railway. When reconstructing railway lines, it is not the traditional elevation level that is used but the elevation of the rail head [8]. The accuracy of the calculations is up to 1 mm. The presence of steel bridges without a ballast bed, open culverts, bridges with a minimum height above the high water level, railroad crossings and stations with intersection of several directions and available industrial branches, determine the level of the new level.

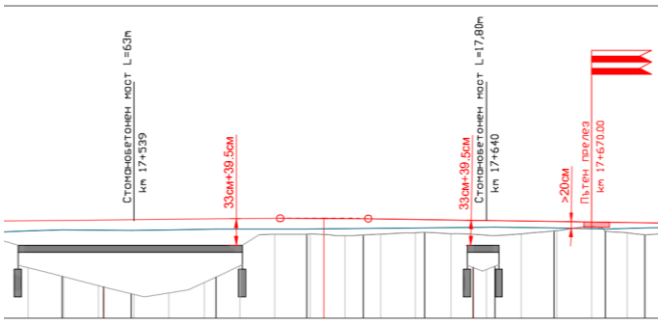

Fig. 2 *Railroad crossing near to reinforced concrete bridge*

Removing the level of the track in the presence of concrete bridges is impossible if the crossing is within walking distance (in this case 20 m). These reinforced concrete bridges require the

presence of 33 cm of ballast over waterproofing and protection and another 7-8 cm of elevation due to alteration of the upper railway track structure. This requires a total of about 24 cm of leveling in comparison to the existing figure 2.

Keeping the level causes problems with the railroad crossing. The approaches of the motor road to the crossing, defined in Ordinances 55 and 58 [9, 10], are changing. The situation is even more difficult if the bridge is steel without a ballast bed.

3. Problems in the situation

When the railroad crossing is in a horizontal curve for the railway, a cant is required in the curve. For small radii the excess is maximum cant. A concrete example is a railroad crossing, which is located in a horizontal curve with a small radius of 298 m and a height of 150 mm - Fig.3.

The Iliyantsi – Kurilo and Kurilo - Ribrovo railway is two-road railways. The cant of both roads is the maximum possible for design speed. This leads to a decrease in the comfort of car traffic, albeit within the capabilities of the rolling stock.

The solution is to reduce the speed of travel. In terms of safety it is good, but reducing the speed of vehicles nervous drivers.

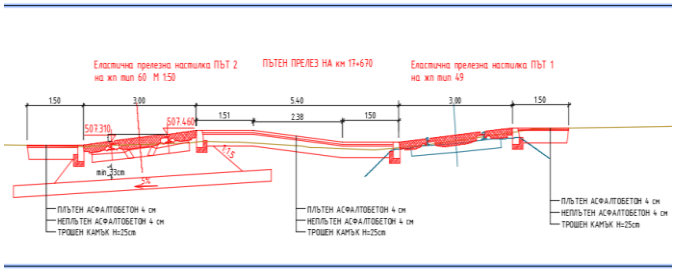

***Fig. 3** Maximum cants of both roads at small radius*

Although not laid down in the assignment, raising the level of the road, new approaches to the crossing would solve the problem - figure 4. If the railway line was one road, the level of the motor road could be changed.

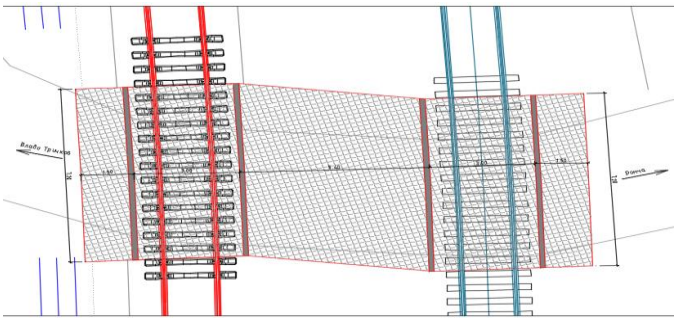

Fig. 4 Changing the straightness of the railroad crossing

The Ordinance on the railroad crossing and the existing Ordinance 55 [10] give the railroad crossing device at a perpendicular and inclined at a certain constant angle the intersection of the railway and the road.

In two line railway, the two pavements may not be parallel. This causes the straightness of the road to be disturbed and the speed of the cars restricted. With existing railroad crossings [11, 12] this is not fatal, although it seriously disrupts safety.

In the two-road railway, the railroad crossing is fully dependent on the levels of the two roads to ensure smooth and trouble-free passage of vehicles through it. In cases where the geometric parameters are not properly selected, there is a violation of the pavement of long wheelbase cars and vehicles and increases the risk of accidents caused by damaged or stuck vehicles.

The design decision of the two-road railway and intersection should be complex, covering the two railway tracks and the asphalt road passing through them.

The solution for changing the level of the two railway tracks and road approaches is the best option figure 5.

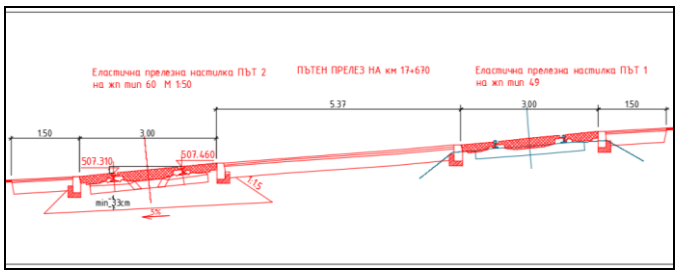

Fig. 5 Synchronization of the levels of the two-road railway

This variant necessitates a change in the levels of Route 1 within about one kilometer, around the railroad crossing. On the one hand, this is not included in the assignment and the quantitative account of the works contract. On the other hand, it is difficult because of the existence of solid points along the railway, which also alter the necessary activities. These can be railway station platforms - requiring height adjustment, bridges - requiring repair of the walls or ballasts or complete replacement of the facility, tunnels, contact network requiring replacement of the pillars, etc. The changed load on rolling stock and road traffic is also irrelevant [13]. In the construction of the motor road more ten years ago, the axle load was one, and now it has changed (increased).

At km 17 + 670, lifting of road 1 is practically impossible due to the presence of a steel bridge with wooden sleepers and without ballast bed 15 m before it, and nailing the level at the crossing to the nearest 1 millimeter. Changing the level of the steel bridge is only possible with major reconstruction of the facility or its replacement.

At the railroad crossing at Novi Iskar railway station on road 1 immediately before the crossing there is a platform, the change of which is also not within the scope of construction works. The height of the platform is a constant relative to the level of the rail head. This defines a solid point for the leveling line.

4. Decisions with a reduction of the cant in railway curve

This decision provides good compromise geometry of the crossing of road vehicles but increases operating costs for track and reduces passenger comfort on it.

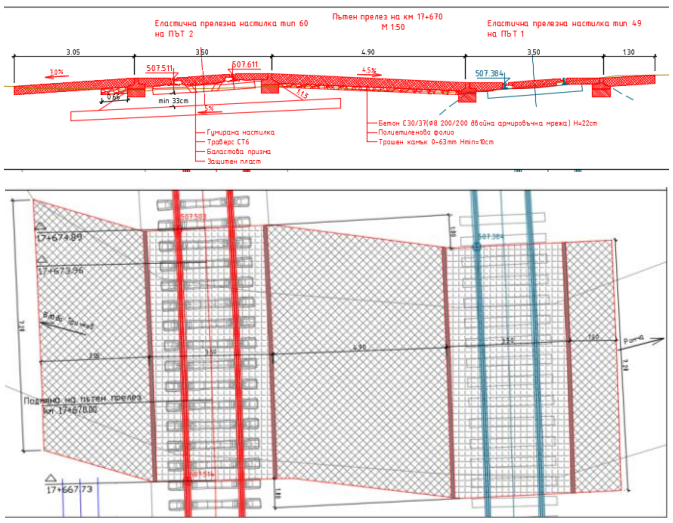

Fig. 6 Compromise reduction of the cant

The decrease of the cant in the crossing zone leads to the appearance of excess and shortage of cant. Normally, in mixed traffic, freight trains experience an excess of cant and passenger trains shortages of cant. The compromise of reducing the required overrun leads to additional checks on the minimum unslaked acceleration for passing trains.

3. References

Restrictive conditions predetermine the railroad crossing of the track in the presence of any compromises. Therefore, it is necessary to look for complex design solutions to balance the situation with regard to road vehicles and, accordingly, to improve it with regard to the railway infrastructure as well, in all cases the safety of the intersection comes first.

The options for solving the problems are:

- Situation analysis;
- Finding working solutions;
- Assessment of the damage and benefits of a decision and economic justification.

The findings and conclusions lead to:

- Making an analysis of possible solutions;
- Economic justification for the options;
- Preventive problem solving;
- Reduction of risks when crossing junctions are needed;
- Preliminary projects and studies to properly assess the need and scope of a repair contract.

***Literature**:*

1. Railway network reference document 2019-2020, Valid from 12/15/2019 to 12/12/2020, Reference Document_2019-2020_v.10_02042020.pdf https://www.rail-infra.bg/bg/139
2. Todorov S., M. Zhiponov, ISPA Infrastructure project Plovdiv - Svilengrad, UACEG International scientific and applied conference 2009, October 29–31, 2009, UACEG Annuals, ISSN 1310-814X (print); ISSN 2534-9759 (online), Scroll XI, Bridges, transportation construction, pp.239-247
3. Todorov S., R. Valkov, Strategic requirements for designing the reconstruction and electrification of sections of the first railway line, Scientific papers 72, Vasil Levski Higher educational military school V. Turnovo, 2002, pp.421-428, ISSN 0861-0312
4. Nikolov V., Todorov S., Pavements for railroad crossings, Railway transport magazine, 1310-683X (print), 3/2001. Sofia, pp.22-24
5. Kostadinov N., S. Todorov, Road safety at the crossing of a railroad crossing, NPP "Traffic Safety", Thracian University, Stara Zagora, TC Yambol, May 11, 2011, ISBN: 978-954-9999-77-8, p. 5-10
6. Ivanova M., S. Todorov, Road traffic safety at Bulgarian railroad crossings, NPP "Traffic Safety", Thracian University, Stara Zagora, TC Yambol, May 11, 2011, ISBN: 978-954-9999-77-8, pp. 11-16
7. Work projects along part of the railway for "Restoration of the design speed in the Kurilo - Rebrovo inter-station, road № 2 from km 13 + 294 to km 23 + 632 with a length of 10 338 m, with adjacent stations: Kurilo station - etc. 2 with a length of 980 m and adjacent turnouts № 8, 10, 14, 9 and 3, between turnouts № 10 and № 14 with a length of 46 m, and between turnouts № 3 and № 9 with a length of 22 m and station Rebrovo - item 2. n 2 with a length of 891 m and adjacent turnouts № 1 and 2 ".
8. Nikolov V., Todorov S., Roads and railways, Printed in VTU "T. Kableshkov ", ISBN 978-954-12-0205-0, 2011, 471 pages
9. Ordinance No. 58 on the rules for the technical operation, movement of trains and signalling in railway transport, issued by the Minister of Transport, promulgated, SG, issue 73 of 5.09.2006, amend. and suppl., issue 43 of 2009, issue 68 of 2014, and issue 97 of 23/11/2018, effective from 24.02.2019.
10. Ordinance No. 55 of January 29, 2004 on the Design and Construction of Railways, Railway Stations, Railway Crossings and Other Elements of the Railway Infrastructure (promulgated, SG No. 18 of 05.03.2004).
11. Rasimova A., S. Todorov, Railroad crossing with barriers Asenovgrad. European trends in road safety, Journal of the Technical University - Sofia, Plovdiv branch, Bulgaria, Fundamental Sciences and Applications Vol. 19, 2013, International Conference Engineering, Technologies and System, TECHSYS 2013, Bulgaria
12. Todorov S., Safety measures for level crossings, 11-th Forum of rail transport, Bratislava, h. Double Tree by Hilton, 17 - 18 March 2015 г., p. 71-75
13. Nikolov V., Todorov S., Ivanov R., Combined impact of rolling stock loading and road traffic on the lane in the area of railroad crossings, Railway Transport Magazine, 1310-683X (print), 5/2000. Sofia, pp. 34-37
14. Todorov S., Train movement in horizontal curves - shortage and excess of cant, Electronic Journal of Mechanics, Transport, Communications, ISSN 1312-3823, Volume 12, Issue 3/3, Year 2014, pp. VIII-9 -15, http://www.mtc-aj.com/academic-journal.php?lang=en

Researching of the factors determinant safety movement of the train in braking regime – impact of braking force on the superstructure of the railway with regard to the interoperability and the experience of the railway section Gorna Oriahovitsa

Kina Kutsarova-Dimitrova
University of Architecture Civil engineering and Geodesy – Sofia, Bulgaria
kina_kutzarowa@abv.bg

Abstract: *The horizontal reaction of the rail is very important to the creation of the braking force. The value of rail reaction is equal to the value of the braking force. The subject of the article is the determination of braking force in two different ways. The first is based on braking pressure for one braking jay and friction between braking jay and wheel for vehicles equipped with block brake. The second is based on braked weight and braked weight percentage. The theoretical results obtained by the two methods are compared on the basis of the need for interoperability under Regulation 1299/2014 relating to Infrastructure subsystem of the rail system of the EU. The practical impact of braking force in declivities with a gradient of slope over 15 ‰ has been established on the basis of direct observations and analyzes. The experience in the operation of heavily inclined sections of the Gorna Oryahovitsa railway section has been used.*
Keywords*: BRAKING FORCE, BRAKING WEIGHT, TRAIN, RAILWAY TRACK, SLOPE-DOWN MOVEMENT*

1. Introduction

The slope-down movement of the train requires the using of braking force to maintain a safety running speed. Applied to the wheel-rail contact plane, this braking force causes a horizontal reaction in the rail and additionally loads the elements of the railway superstructure. For the design of railway lines, this braking force can be determined using approximate methods. The calculation of the braking force is done in an easy-to-apply manner based on the friction between the cast-iron brake shoes and the wheel. This method is different from the requirements for calculation of the braking force based on braked weight and braked weight percentage given in UIC methodology. The comparison of calculation methods of braking force would be useful in terms of updating and technical harmonization of the principles of designing railway lines. The other side of the examination is the effect that the braking force has on the elements of the upper structure. The other side of the examination is the effect of the braking force on the elements of the superstructure. The impact can be assessed on the base of direct observations, data collection, and analysis of road conditions in heavily inclined sections.

2. Comparison of the methods for determining braking force. Determine the additional load on the superstructure of the track that it causes

2.1. Determination of braking force based on the friction between the cast iron brake shoes and the wheel

The pressure of the brake shoes on the wheels of one brake axle causes friction force [1, 2]. The internal force pair BB_1 appears (fig.1). The force transmitted on the rail is B_1. B_1 is limited by the force of adhesion.

(1) $B_1 = K\varphi_k$ [1, 2]

Where K [KN/axle] – pressure for one brake axle; φ_k – factor of friction brake shoes and wheel.

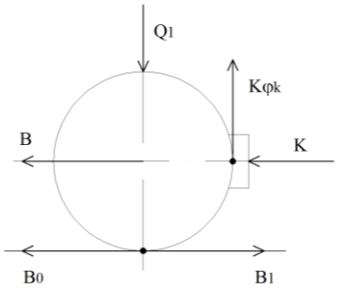

Fig.1 *Creating of the braking force*

The B_1 force causes the reactive external force B_0 and they balance each other. Only force B remains to act, but it is conditioned by the appearance of B_0. The force B_0 is limited by the adhesion force by K and φk.

(2) $B_0 = 10K\varphi_k \le 10\psi Q_1$

Where: B_0 [kN] – rail reaction; Q_1 [t] – weight for one axle; ψ - factor of cohesion between wheel and rail.

The factor φ_k depends on the speed, the pressure of one brake shoe and the material of the friction surfaces. The factor φ_k is the connection between speed and brake force.

(3) $\varphi_k = 0.6\,\frac{1.6k+100}{8k+100}\,\frac{V+100}{5V+100}$

Where: k [kN] – brake pressure of one brake block; V [km/h] – speed.

The full braking force B_k [kN] for the train as a whole is:

(4) $B_k = \sum B_0 = 10\sum K\varphi_k$

Where: B_k [kN] – full braking force; B_0 [kN] – sum of rail reaction for all braking axles; ΣK [kN] – total pressure force for the whole train; φ_k – factor of friction brake shoes and wheel.

Equation (4) can be used to calculate the full braking force of a train with the same braking equipment for all wagons. Calculating the braking force is more complicated for a train composed of wagons with different braking equipment. Average values of friction factor and pressure of one brake axle are used for easier calculation.

The described method makes it possible to calculate the additional load on the superstructure of the track caused by the reaction of the rail ΣB_0 at the moment of acting of braking force.

2.2. Determination of the braking force by the brake weight and the brake weight percentage

2.2.1. Braking performance according to UIC 544-1

Assessing the braking performance according to [3] are the brake weight B and the braked weight percentage λ. Braked weight percentage depends on stopping distance and speed and assessment diagrams are given. The reference train was equipped with block brakes with low-phosphorus cast-iron blocks.

The braking weight of wagon fitted with cast iron brake blocks maximum speed ≤120km/h, and maximum axle load 22.5t can be determined [3] by using equation (5):

(5) $B = \frac{k\sum Fdyn}{g}$

Where: B[t] braking weight; k – assessment factor for determining the braked weight; ΣFdyn [kN] – sum of all brake block forces during the run; g=9.81m/s^2 – gravity acceleration.

The values of one brake block forces during the run for 2-axil and 4-axil wagons is given in [3].

2.2.2. Determination of braking force

Equation (4) can be used to calculate the brake force if total pressure force for the whole train ΣK is known. The brake weight of wagon can be used to calculate the total pressure force of brake axles. The total brake pressure of wagon is:

$$(6)\ \sum K_1 = \frac{B}{\chi}\ [4]$$

Where: ΣK_1[t] – total pressure force of one wagon; B[t] – brake weight; χ – empirical coefficient.

Substituting braking weight B from equation (5) for total pressure force is obtained:

$$(7)\ \sum K_1 = \frac{k\sum Fdyn}{\chi}$$

Where: ΣK_1 [kN] – total pressure force of one wagon.

The total braking pressure for the train as a whole is:

$$(8)\ \sum K = \sum\sum K_1 = \sum \frac{k\sum Fdyn}{\chi}$$

Where: ΣK [kN] – total pressure force of the train.

The full braking force is:

$$(9)\ B_k = \sum B_0 = \varphi_k \sum \frac{k\sum Fdyn}{\chi}$$

In regulation 58 [5] are given the braking percentages according to the slope. Regulation 58 is harmonized [6] with UIC code 544-1.

3. Analysis of train running and permissible (allowable) speed as a function of railway track inclination

The diagram of the resultant relative force in a braking regime of moving (fig. 2) can be used to analyze the train movement and the allowable speed as a function of the track slope. Braking regime is used to maintain a fixed, constant speed of train movement [7]. The resultant relative force in a braking regime is [8]:

$$(10)\ r_b = r_m + \alpha b_k$$

Where: r_b [dN/t] - the resultant relative force in braking regime; r_m [dN/t] - the resultant relative force in mechanical regime; b_k [dN/t] – relative braking force; α - factor for intensity of braking process (α=1 for rapid brake)

$$(11)\ b_k = 100\frac{B_k}{P+Q}$$

Where: B_k [kN] – full braking force; P[t] – locomotive weight; Q[t] – wagons weight.

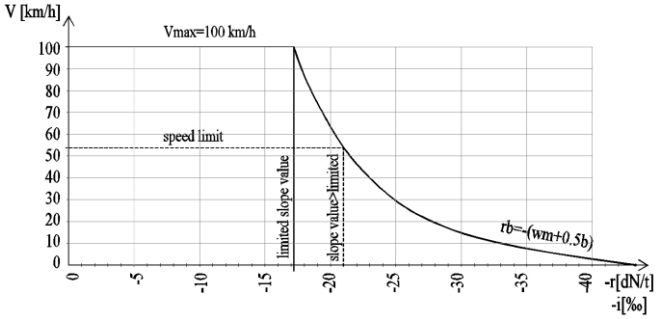

Fig.2 *Diagram of resultant relative force in braking regime*

The Diagram of resultant relative force in a braking regime (fig. 2) for a given railway line gives the limited slope value for maximum speed for every train. For slopes greater than the limited slope, it is necessary to reduce speed because of brake not because of the track geometry.

For example, Vakarel - Verinsko section with slope value 25‰, maximum speed 100km/h [9] has limited speed by braking 45km/h.

The limit of speed increase traveling time. It is concluded that in order to increase speed, it is necessary to limit the slope values. According to [10] the slope of the moving average profile over 10 km is less than or equal to 25mm/m (25‰).

4. Impact of braking force on the superstructure of the railway with regard to the experience of the railway section Gorna Oriahovitsa

Sections in big acclivity are used to overcome difficult terrain conditions. These sections are often combined with horizontal curves with small radii in a situation. For example: the sections of the 4 railway line Borovo - Morunitsa from km 62+417 to km 65+585 with slopes between 21 and 27 ‰ and radii of curves between 250 and 355m and the section Plachkovtsi - Krastets from km 185+400 to km 192+945 s slopes between 17 and 26 ‰ and radii of curves between 275 and 300m. There is more intensive wear of the rails at the horizontal curves with small radii. Lubricants are used to reduce wear and tear, but the cohesion between the wheel and the rail is reduced too and braking is difficult. Very precise dosing of the lubricant is required, and nevertheless, there are registered problems.

Another problem is the danger of igniting from transfer flying sparks. Such cases are registered in the section Morunica - Byala, where the rails lie on timber sleepers. Ignition is caused by sparks from the braking block of freight trains.

The joints are shifted in the direction of the slope and often the connection between the rails displaces beyond the zone of the sleeper. This is very difficult to repair within the current track maintenance. The problems with rotated sleepers and slipping of joints are increasing in sections in big declivities with heavy freight traffic. There are problems not only when the train moves down to the slope but and when a train moves in the opposite direction (acclivity). There is very big wear of the rails in these profile sections (fig. 3).



Fig.3 *Wear of the rails in section with big longitudinal slope*

5. Conclusion

The method of calculating the braking force taught so far at UACEG can be successfully updated by using the braking weight and braking weight percentage given in recommendations of UIC code 544-1. The following can be said about analyze train movement in braking regime:

1. Braking regime is used not only when braking is necessary, but also to maintain a safe speed of moving.
2. By increasing the slope, the permissible speed because of a brake is reduced.
3. The speed limit is the reason for the increase of travel time in the steep track sections.

The adverse effect of the braking force on the superstructure of the railway is increasing by increasing the slope. It is necessary for the railway superstructure to be with more reliability construction in these sections.

6. Literature

1. Димитров Т., Йо. Тотев, М. Събев. Железопътно строителство. София, УАСГ, 1991, 386 стр. (Dimitrov T., J. Totev, M. Sabev. Railway engineering)

2. Тодоров Ст. Проектиране и строителство на жп линии. София, УАСГ, 2006, 334 стр. (Todorov St. Design and construction of railway lines)

3. UIC CODE 544-1: Brakes – Braking performance. 6th edition, October 2014

4. Пургич С. Усъвършенствани алгоритми за енергийно ефективно управление на тяговия подвижен железопътен състав – автореферат. София, ТУ, 2014, 32 стр.

5. Наредба 58 от 2.08.2006 г. за правилата за техническата експлоатация, движението на влаковете и сигнализацията в железопътния транспорт, издадена от министъра на транспорта, обн., ДВ, бр.73 от 5.09.2006 г., изм., бр.88 от 2007 г., изм. и доп., бр.43 от 2009 г., бр.68 от 2014 г., и бр.97 от 23.11.2018 г., в сила от 24.02.2019 г.

6. Todorov S. Research of the factors determining the safety of train movement under braking - interoperability, 4-th international scientific conference – winter session Industry 4.0 11-14.12.2019 Borovets, ISSN 2535-0153 (Print), ISSN 2535-0161 (Online).

7. Тодоров С., К. Куцарова. Определяне на спирачната сила и оценка на опасните участъци по жп мрежата на РБ. - XXIV международна научна конференция „Транспорт 2019“, на ВТУ „Т. Каблешков“, списание „Механика Транспорт Комуникации”, ISSN 1312-3823 (print), ISSN 2367-6620 (online), бр. 3, 2019, стр. VIII-19- VIII-24 (Todorov S., K. Kutsarova. Determination of braking force and assessment of dangerous sections of the railway network of the Republic of Bulgaria)

8. Dencheva Z., K. Kutzarova-Dimitrova, Railway engineering, textbook for University of Architecture, Civil engineering and Geodesy, ISBN978-954-724-116-9, 2018, p. 139

9. Таблици с технически параметри и нормативи, приложение към книжка разписание, в сила от 09.12. 2018 до 14.12.2019г.

10. COMMISSION REGULATION (EU) No 1299/2014 of 18 November 2014 on the technical specifications for interoperability relating to the ‘infrastructure’ subsystem of the rail system in the European Union.

The change in energy flow streams for main marine propulsion steam turbine at different loads

Mrzljak Vedran, Prpić-Oršić Jasna, Medica-Viola Vedran, Anđelić Nikola
Faculty of Engineering, University of Rijeka, Vukovarska 58, 51000 Rijeka, Croatia
E-mail: vedran.mrzljak@riteh.hr, jasna.prpic-orsic@riteh.hr, vmedica@riteh.hr, nandelic@riteh.hr

Abstract: *This paper present analysis of energy flow streams through the main steam turbine (the turbine is used for commercial LNG carrier propulsion) at three different loads. An increase in the propulsion plant (and proportionally increase in the main turbine) load resulted with an increase in energy flow streams and with an increase in the amount of water droplets inside steam at the main turbine outlet. Analyzed turbine has three steam extractions which opening as well as the amount of energy flow stream delivered through each extraction, significantly differs at various loads. The analysis shows that the highest energy flow stream consumers from the main turbine are deaerator and high pressure feed water heating system.*

KEYWORDS*: MAIN MARINE STEAM TURBINE, ENERGY FLOW STREAMS, LOAD CHANGE, POWER DISTRIBUTION*

1. Introduction

In a worldwide fleet, the dominant power producers for ship propulsion are nowadays internal combustion engines [1-3]. Steam and gas turbines are usually rarely used, but however, they have application in engine rooms of a certain ship types [4] and they are (or can be) a baseline for new complex marine propulsion plants [5, 6].

In propulsion of LNG carriers, steam propulsion plants still have a dominant role caused by its operation specificity and characteristics of transported cargo [7, 8], but also, the internal combustion engines impact in this ship type is each day more and more evident [9].

This paper presents analysis of energy flow streams through main marine propulsion steam turbine, which operates at the LNG carrier. Analysis was performed at three different turbine loads. It is analyzed and explained the dynamics in energy flow streams change during the change in turbine load, and the influences of such change on the entire marine propulsion plant operation are discussed. At the end is presented cumulative produced power distribution at each turbine cylinder (for each observed turbine load) and the guidelines for a future research are provided.

2. Description and operating characteristics of main marine propulsion steam turbine

Main marine propulsion steam turbine analyzed in this study is used for the conventional LNG carrier drive. The main specifications of the LNG carrier are presented in [10]. Turbine consists of two cylinders - HPC (High Pressure Cylinder) and LPC (Low Pressure Cylinder), Fig. 1. Both turbine cylinders are connected to a gearbox, through which is obtained propulsion propeller drive.

The marine steam propulsion plant has two identical steam generators (due to safety reasons). Cumulative produced steam mass flow rate is mainly delivered to all turbines which exist inside the power plant (main propulsion turbine, turbogenerators and steam turbine for the main feed water pump drive [11, 12]), while one smaller amount of steam (with reduced temperature) is delivered to other ship systems (auxiliary steam).

Steam delivered to the main propulsion turbine expanded firstly through HPC and after expansion in HPC, steam is delivered directly to LPC (analyzed steam turbine did not posses steam reheating like newer versions of such turbines [13]). After expansion in LPC, steam is delivered to the main marine steam condenser.

Entire main marine propulsion steam turbine has three steam extractions, as presented in Fig. 1. First extraction is from HPC (extracted steam is used for ship auxiliary systems heating), second extraction is located between HPC and LPC (extracted steam is used for steam delivery into the deaerator and high pressure feed water heating system); while third extraction is from LPC (extracted steam is used for heating low pressure condensate heating system components). It should be noted that steam extractions opening/closing as well as steam mass flow rate extracted from each extraction depend on current steam propulsion plant load (steam propulsion plant load is proportional to main propulsion turbine load). Also, in this analysis, steam mass flow rates lost through both gland seals of each main propulsion steam turbine cylinder are neglected [14] in order to present the change of dominant energy flow streams through turbine at different loads.

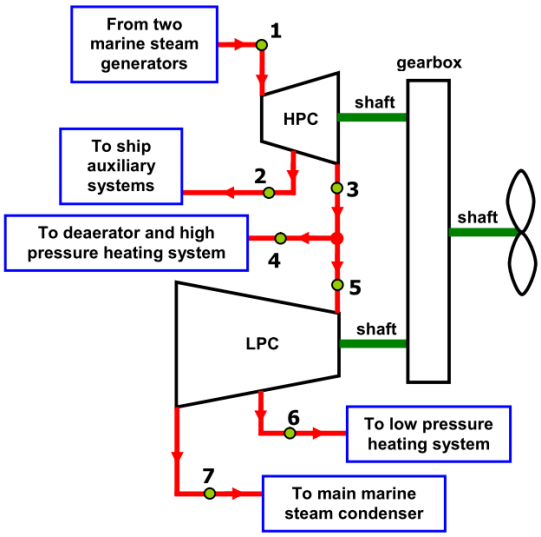

Fig. 1. *Main marine propulsion steam turbine with operating points required for the analysis*

3. Governing equations required for the analysis

All of the equations in this section are based on the observed main marine propulsion steam turbine and its operating points presented in Fig. 1.

Energy analysis of any plant, system or a component is based on the first law of thermodynamics [15, 16]. The main energy balance equation can be expressed as presented in [17]:

$$\left(\dot{Q}+P+\sum(\dot{m}\cdot h)\right)_{\text{input}}=\left(\dot{Q}+P+\sum(\dot{m}\cdot h)\right)_{\text{output}}, \quad (1)$$

where $\dot{Q}$ is heat transfer in kW, P is power in kW, $\dot{m}$ is operating medium mass flow rate in kg/s and h is operating medium specific enthalpy in kJ/kg.

For any fluid stream (for each operating point in Fig. 1), energy flow is calculated as presented in [18]:

$$\dot{E}_{\text{en}}=\dot{m}\cdot h, \quad (2)$$

where $\dot{E}_{\text{en}}$ in kW is energy flow of any fluid (operating medium) stream.

HPC developed power in each turbine load is calculated as:

$$P_{\text{HPC}}=\dot{m}_1\cdot(h_1-h_2)+(\dot{m}_1-\dot{m}_2)\cdot(h_2-h_3), \quad (3)$$

while LPC developed power in each turbine load is calculated as:

$$P_{LPC} = \dot{m}_5 \cdot (h_5 - h_6) + (\dot{m}_5 - \dot{m}_6) \cdot (h_6 - h_7) . \quad (4)$$

Cumulative produced power for the main propulsion propeller drive (cumulative power produced by the main turbine) is:

$$P_{cumulative} = P_{HPC} + P_{LPC} . \quad (5)$$

The share of each cylinder in cumulative main marine propulsion steam turbine developed power is:

$$Z_{HPC}(\%) = \frac{P_{HPC}}{P_{cumulative}} \cdot 100 = \frac{P_{HPC}}{P_{HPC} + P_{LPC}} \cdot 100 , \quad (6)$$

for HPC, while this share for LPC is:

$$Z_{LPC}(\%) = \frac{P_{LPC}}{P_{cumulative}} \cdot 100 = \frac{P_{LPC}}{P_{HPC} + P_{LPC}} \cdot 100 . \quad (7)$$

4. Measured steam operating parameters at different loads

For the accurate and precise analysis of energy flow streams through main marine propulsion steam turbine, at each observed load are required steam mass flow rates, pressures and temperatures in each turbine operating point from Fig. 1. Such steam operating parameters are presented in Table 1 for low turbine load, in Table 2 for middle turbine load and in Table 3 for high turbine load [19]. Presented steam operating parameters are measured during marine steam propulsion plant operation by using calibrated measuring equipment which is mounted inside engine room and is used for power plant regulation and control [20].

Along with steam mass flow rates, pressures and temperatures, in Table 1, Table 2 and Table 3 are presented specific enthalpies for each steam flow stream, calculated by using NIST REFPROP 9.0 software [21]. Analysis of energy flow streams is not dependable on the conditions of the ambient in which observed steam turbine operates, therefore the ambient temperature and pressure do not have to be defined [22, 23].

Table 1. *Steam operating parameters at low turbine load*

Low load (Operating points - Fig. 1.)	Temperature (°C)	Pressure (MPa)	Mass flow rate (kg/h)	Specific enthalpy (kJ/kg)
1	488.0	6.190	16605	3392.2
2	-	-	0	-
3	243.0	0.151	16605	2958.8
4	-	-	0	-
5	243.0	0.151	16605	2958.8
6	-	-	0	-
7	32.50	0.00489	16605	2531.7

Table 2. *Steam operating parameters at middle turbine load*

Middle load (Operating points - Fig. 1.)	Temperature (°C)	Pressure (MPa)	Mass flow rate (kg/h)	Specific enthalpy (kJ/kg)
1	513.5	6.020	65012	3454.9
2	-	-	0	-
3	256.0	0.467	65012	2974.6
4	256.0	0.467	4690	2974.6
5	256.0	0.467	60322	2974.6
6	156.0	0.097	2032	2788.7
7	29.47	0.00412	58290	2390.0

Table 3. *Steam operating parameters at high turbine load*

High load (Operating points - Fig. 1.)	Temperature (°C)	Pressure (MPa)	Mass flow rate (kg/h)	Specific enthalpy (kJ/kg)
1	500.0	5.899	96474	3424.3
2	350.0	1.565	3268	3146.7
3	256.0	0.593	93206	2970.4
4	256.0	0.593	13609	2970.4
5	256.0	0.593	79597	2970.4
6	153.0	0.121	3355	2781.1
7	34.92	0.00561	76242	2373.4

5. Results and discussion

All energy flow streams (energy of steam and each cylinder produced power) for the main marine propulsion steam turbine at low load are presented in Fig. 2. The steam energy flow stream which enters in the main turbine from marine steam generators at low load is equal to 15646.52 kW. That steam energy flow stream at low load is used only for power production in HPC and LPC, because all steam extractions (from HPC, from LPC and between cylinders) are closed and energy flow through each extraction is equal to 0 kW. Therefore, it can be concluded that at low load, steam generators produce steam energy flow stream sufficient only for power production by both main turbine cylinders.

At low propulsion plant loads, steam required for all marine elements operation is delivered from steam generators (auxiliary steam), not from main turbine [24]. Steam energy flow stream which is, at low load, delivered to the main marine steam condenser (at the LPC outlet) equals 11677.46 kW and can be calculated as inlet steam energy flow stream (delivered from steam generators) reduced for the produced power of both main turbine cylinders.

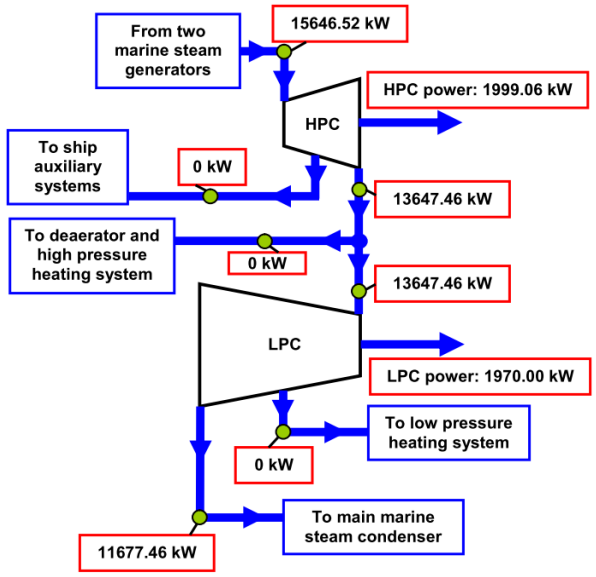

Fig. 2. *Energy flow streams through main marine propulsion steam turbine - low load*

The steam energy flow stream which enters in the main turbine from marine steam generators at middle load is significantly higher in comparison to low load (62391.66 kW in comparison to 15646.52 kW), Fig. 3. Such higher steam energy flow stream is used for much higher power production of both steam turbine cylinders when compared to low load. In addition, at middle load are open two of three steam extractions.

HPC steam extraction is still closed at middle load, so steam for ship auxiliary systems is still delivered from steam generators (auxiliary steam). Steam extractions between two main turbine cylinders as well as LPC extraction are open and cumulative steam energy flow stream extracted from the main turbine at low load is

equal to 5449.31 kW, Fig. 3. From Fig. 3 should be noted that deaerator and high pressure feed water heating system requires more than double steam energy in comparison to low pressure condensate heating system at middle load. Steam energy flow stream delivered to main marine steam condenser at middle load is equal to 38698.09 kW.

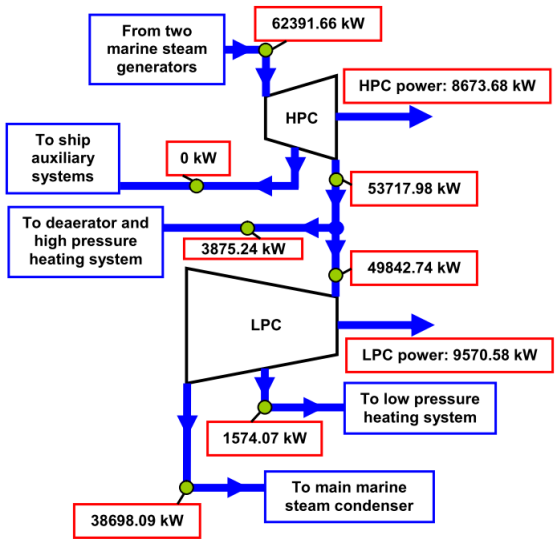

Fig. 3. *Energy flow streams through main marine propulsion steam turbine - middle load*

At high propulsion plant load, steam energy flow streams delivered into the main turbine form steam generators (91765.53 kW) and delivered from main turbine to main marine condenser (50264.66 kW) are the highest in comparison with lower loads, Fig. 4. Also, at high load both main turbine cylinders produce significantly higher power when compared to lower loads.

High propulsion plant load is characterized with a fact that all of three steam extractions are open, and steam is delivered to almost all steam plant components directly from the main steam turbine. Comparison of steam energy flow steams extracted through each main turbine extraction at high load shows that the highest steam energy flow consumers are deaerator and high pressure feed water heating system elements which uses four (or more than four) times higher steam energy flow stream than other extractions. At the same time, ship auxiliary systems and low pressure condensate heating system use steam energy flow streams equal to 2856.50 kW and 2591.83 kW, respectively.

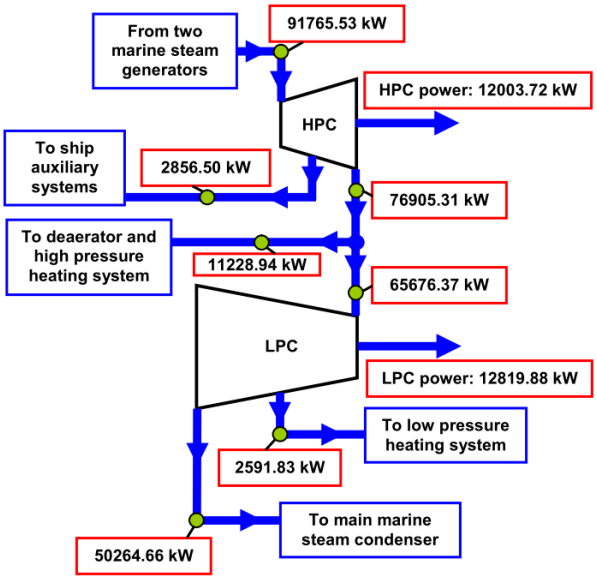

Fig. 4. *Energy flow streams through main marine propulsion steam turbine - high load*

From the previous observations can be concluded that power produced by main marine propulsion steam turbine cylinders increases in each cylinder during the increase in steam plant load. It is interesting to observe the share of each main turbine cylinder in cumulative produced power. In Fig. 5 is presented that at low propulsion plant loads, the dominant power producer inside the main turbine is HPC, while an increase in steam plant load resulted with a fact that at middle and high loads the dominant power producer is LPC. The highest difference between the main turbine cylinders share in cumulative produced power can be seen at the middle power plant load where HPC takes a share of 47.54%, while the LPC takes a share of 52.46%.

Proper main steam turbine operation significantly depends on the proper operation of the main steam condenser. Steam in each operating point of main marine steam turbine from Fig. 1 is superheated with an exception of operating point 7 (entrance into the main condenser) where the steam is saturated, regardless of the observed steam plant load. For the proper main condenser operation is interesting to note that an increase in steam propulsion plant load resulted with a decrease in steam content at the main condenser entrance (LPC outlet). This element resulted with a fact that increase in steam propulsion plant load resulted with higher amount of water droplets inside steam at the last LPC stages and at the main condenser inlet, which is valuable information for designing and maintenance of both main steam turbine and main steam condenser.

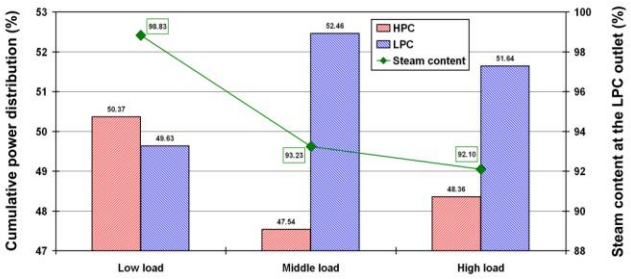

Fig. 5. *Cumulative produced power distribution on both main marine propulsion steam turbine cylinders and steam content at the LPC outlet for all observed loads*

Based on the previous researches of the same authors, further improvement and possible optimization of presented main marine propulsion steam turbine will be performed by using advanced artificial intelligence methods and algorithms [25, 26].

6. Conclusions

This paper presents an analysis of energy flow streams through the main propulsion steam turbine at three different loads. The analysis is based on measured steam operating parameters from conventional LNG carrier on which observed turbine operates (the main turbine is used for LNG carrier propulsion). The main conclusions obtained in this analysis are:

- Energy flow streams notably increases during the increase in propulsion plant load.
- At low propulsion plant loads, all steam extractions from the main turbine are closed. Increase in propulsion plant load resulted with the opening of some steam extractions (middle loads), while at high loads all steam extractions from the main turbine are opened.
- Energy flow streams delivered from main turbine to the steam consumers (through extractions) significantly differs. The highest energy flow stream consumers are deaerator and high pressure feed water heating system.
- At low propulsion plant loads the highest share in cumulative main turbine produced power takes High Pressure Cylinder (HPC), while the dominant power producer at other loads is Low Pressure Cylinder (LPC).
- Increase in propulsion plant load resulted with higher amount of water droplets inside steam at the LPC outlet (main condenser inlet).
- This analysis will be used as a baseline for further research of presented main propulsion steam turbine and for the possible

improvement of the whole propulsion plant in which main turbine operates.

7. Acknowledgment

This research has been supported by the Croatian Science Foundation under the project IP-2018-01-3739, CEEPUS network CIII-HR-0108, European Regional Development Fund under the grant KK.01.1.1.01.0009 (DATACROSS), University of Rijeka scientific grant uniri-tehnic-18-275-1447 and University of Rijeka scientific grant uniri-tehnic-18-18-1146.

8. References

[1] Huang, H., Lv, D., Zhu, J., Zhu, Z., Chen, Y., Pan, Y., Pan, M.: *Development of a new reduced diesel/natural gas mechanism for dual-fuel engine combustion and emission prediction*, Fuel 236, p. 30-42, 2019. (doi:10.1016/j.fuel.2018.08.161)

[2] Senčić, T., Mrzljak, V., Blecich, P., Bonefačić, I.: *2D CFD Simulation of Water Injection Strategies in a Large Marine Engine*, Journal of Marine Science and Engineering 7 (9), 296, 2019, (doi:10.3390/jmse7090296)

[3] Baldi, F., Ahlgren, F., Van Nguyen, T., Thern, M., Andersson, K.: *Energy and Exergy Analysis of a Cruise Ship*, Energies 11, 2508, 2018. (doi:10.3390/en11102508)

[4] Mrzljak, V., Mrakovčić, T.: *Comparison of COGES and diesel-electric ship propulsion systems*, Journal of Maritime & Transportation Sciences-Special edition No. 1, p. 131-148, 2016. (doi:10.18048/2016-00.131)

[5] Fernández, I. A., Gómez, M. R., Gómez, J. R., Insua, A. A. B.: *Review of propulsion systems on LNG carriers*, Renewable and Sustainable Energy Reviews 67, p. 1395–1411, 2017. (doi:10.1016/j.rser.2016.09.095)

[6] Chang, D., Rhee, T., Nam, K., Chang, K., Lee, D., Jeong, S.: *A study on availability and safety of new propulsion systems for LNG carriers*, Reliability Engineering and System Safety 93, p. 1877– 1885, 2008. (doi:10.1016/j.ress.2008.03.013)

[7] Attah, E. E., Bucknall, R.: *An analysis of the energy efficiency of LNG ships powering options using the EEDI*, Ocean Engineering 110, part B, p. 62-74, 2015. (doi:10.1016/j.oceaneng.2015.09.040)

[8] Ammar, N. R.: *Environmental and cost-effectiveness comparison of dual fuel propulsion options for emissions reduction onboard LNG carriers*, Shipbuilding 70 (3), p. 61-77, 2019. (doi:10.21278/brod70304)

[9] Raptotasios, S. I., Sakellaridis, N. F., Papagiannakis, R. G. Hountalas, D. T.: *Application of a multi-zone combustion model to investigate the NOx reduction potential of two-stroke marine diesel engines using EGR*, Applied Energy 157, p. 814-823, 2015. (doi:10.1016/j.apenergy.2014.12.041)

[10] Mrzljak, V., Poljak, I., Mrakovčić, T.: *Energy and exergy analysis of the turbo-generators and steam turbine for the main feed water pump drive on LNG carrier*, Energy Conversion and Management 140, p. 307–323, 2017. (doi:10.1016/j.enconman.2017.03.007)

[11] Behrendt, C., Stoyanov, R.: *Operational characteristic of selected marine turbounits powered by steam from auxiliary oil-fired boilers*, New Trends in Production Engineering 1 (1), p. 495-501, 2018. (doi:10.2478/ntpe-2018-0061)

[12] Mrzljak, V., Prpić-Oršić, J., Poljak, I.: *Energy Power Losses and Efficiency of Low Power Steam Turbine for the Main Feed Water Pump Drive in the Marine Steam Propulsion System*, Journal of Maritime & Transportation Sciences 54 (1), p. 37-51, 2018. (doi:10.18048/2018.54.03)

[13] Koroglu, T., Sogut, O. S.: *Conventional and Advanced Exergy Analyses of a Marine Steam Power Plant*, Energy 163, p. 392-403, 2018. (doi:10.1016/j.energy.2018.08.119)

[14] Lorencin, I., Anđelić, N., Mrzljak, V., Car, Z.: *Exergy analysis of marine steam turbine labyrinth (gland) seals*, Scientific Journal of Maritime Research 33 (1), p. 76-83, 2019. (doi:10.31217/p.33.1.8)

[15] Kanoğlu, M., Çengel, Y.A., Dincer, I.: *Efficiency Evaluation of Energy Systems*, Springer Briefs in Energy, Springer, 2012. (doi:10.1007/978-1-4614-2242-6)

[16] Yoru, Y., Karakoc, T. H., Hepbasli, A.: *Dynamic energy and exergy analyses of an industrial cogeneration system*, International journal of energy research 34, p. 345–356, 2010. (doi:10.1002/er.1561)

[17] Ahmadi, G. R., Toghraie, D.: *Energy and exergy analysis of Montazeri Steam Power Plant in Iran*, Renewable and Sustainable Energy Reviews 56, p. 454–463, 2016. (doi:10.1016/j.rser.2015.11.074)

[18] Cengel Y., Boles M.: *Thermodynamics an engineering approach*, Eighth edition, McGraw-Hill Education, 2015.

[19] Mrzljak, V., Poljak, I., Medica-Viola, V.: *Dual fuel consumption and efficiency of marine steam generators for the propulsion of LNG carrier*, Applied Thermal Engineering, 119, p. 331–346, 2017. (doi:10.1016/j.applthermaleng.2017.03.078)

[20] Mrzljak, V., Poljak, I.: *Energy Analysis of Main Propulsion Steam Turbine from Conventional LNG Carrier at Three Different Loads*, International Journal of Maritime Science & Technology "Our Sea" 66 (1), p. 10-18, 2019. (doi:10.17818/NM/2019/1.2)

[21] Lemmon, E.W., Huber, M.L., McLinden, M.O.: *NIST reference fluid thermodynamic and transport properties - REFPROP*, version 9.0, User's guide, Colorado, 2010.

[22] Mrzljak, V., Blecich, P., Anđelić, N., Lorencin, I.: *Energy and Exergy Analyses of Forced Draft Fan for Marine Steam Propulsion System during Load Change*, Journal of Marine Science and Engineering 7, 381, 2019. (doi:10.3390/jmse7110381)

[23] Blažević, S., Mrzljak, V., Anđelić, N., Car, Z.: *Comparison of energy flow stream and isentropic method for steam turbine energy analysis*, Acta Polytechnica 59 (2), p. 109–125, 2019. (doi:10.14311/AP.2019.59.0109)

[24] Mrzljak, V., Prpić-Oršić, J., Senčić, T.: *Change in Steam Generators Main and Auxiliary Energy Flow Streams During the Load Increase of LNG Carrier Steam Propulsion System*, Scientific Journal of Maritime Research 32 (1), p. 121-131, 2018. (doi:10.31217/p.32.1.15)

[25] Lorencin, I., Anđelić, N., Mrzljak, V., Car, Z.: *Multilayer Perceptron approach to Condition-Based Maintenance of Marine CODLAG Propulsion System Components*, Scientific Journal of Maritime Research 33 (2), p. 181-190, 2019. (doi:10.31217/p.33.2.8)

[26] Lorencin, I., Anđelić, N., Mrzljak, V., Car, Z.: *Genetic Algorithm Approach to Design of Multi-Layer Perceptron for Combined Cycle Power Plant Electrical Power Output Estimation*, Energies 12 (22), 4352, 2019. (doi:10.3390/en12224352)

Methodology for static tuning of the HEV fuel flow measuring system

Slavcho Bozhkov[1], Georgi Tonkov[2]

[1]Department of Transport Equipment, [2]PhD student, Todor Kableshkov University of Transport, Bulgaria
E-mail: stbozhkov@vtu.bg, tonkov.smolyan@gmail.com

Abstract: *The modern automobiles are subject of more stringent requirements [1] corresponding to power, torque, fuel economy and ecology legislations, which is led to designing of new power sources and constructions, such as the hybrid electric vehicles (HEV). They are moving by the energy [2], which is ensured by the internal combustion engine (ICE) and the battery. The main factor in this area is the HEV fuel system, which is controlled by the electronic control unit (ECU) [1]. The electronic control of the Spark Ignition Engines (SI engines), as well as the Direct Ignition Engines (DI engines) is based on the certain sensors signals, program maps and management algorithms. The result in this electronic control is the management of the fuel injectors. The management of the fuel injectors consists in the start of injection, injection duration, number of injection events, injection advance, injection pressure etc. Moreover, the fuel consumption and fuel efficiency are the main factors, which are determining the HEV advances. The learning and measuring the HEV fuel consumption, as well as, the conventional automobiles, is the ground for achievement of quality results in the education of the automotive engineers, as well as for obtaining of scientific researching for developments and innovations. Significant meaning in this concept has the real, live and practical performance with the help of testing equipment and test-benches. This paper renders the methodology of static tuning the Fuel Flow Measuring System EFMS100 on the test bench SAV-1 with the support of controller Matrix MIAC MI0245 and Flowcode 7 software.*

Keywords*: HEV, FUEL FLOW, METERING, METHODOLOGY*

1.Introduction

The hybrid electric vehicles or simply hybrid vehicles use both electric motors and an SI engine for delivering the propulsion power [3]; these vehicles have lower emissions compared to a similarly sized conventional vehicle, resulting in less environmental pollution. The ICE used in a HEV is, of course, downsized compared to an equivalent vehicle engines. The SI engine in combination with the electric motor and an energy storage unit battery provide an extended range for HEV and bring down pollution. The HEV serves as a compromise for the environmental pollution problem and the limited range capability of today's purely electric vehicle (EV). The HEV energy efficiency is the main factor for its advantage and evaluating. This efficiency depends directly from the HEV fuel consumption. It is very important to measure the fuel consumption in correct manner and with suitable equipment to obtain the correct results. Meanwhile, the fuel consumption metering equipment must be calibrated and adapted to the current tests.

2.Structure

The fuel consumption metering equipment is specialized set of fuel sensors, metering units and display units. I accordance with the fuel to use there is different kind of sensors and metering techniques. In this case the EFMS100 [4] metering system is used. It consists from two sets of fuel sensors, metering units and display units (fig.1).

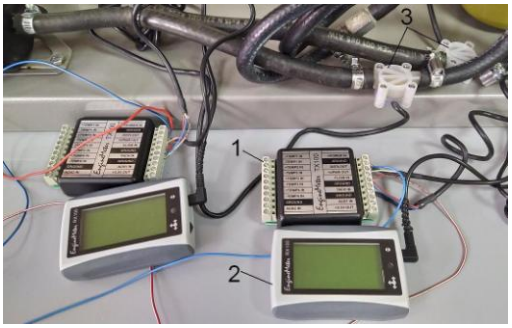

Fig.1 *EFMS fuel flow metering system [4]: 1-metering unit; 2-display unit; 3-fuel flow sensor*

The fuel metering system must be calibrated according to the amount of the fuel flow in the current application. In the case of metering the HEV fuel consumption it is very useful to apply test benches, which can adjust and calibrate the equipment according to the flow range. Such test bench is the test bench SAV-1 [5] for automated management of the automotive gasoline fuel injectors SAV-1 (fig.2). The test-bench can be programmed and managed by the Flowcode 7 software [6], which ensures adjustment to the real work mode of the fuel injectors in the modern automobiles and HEVs.

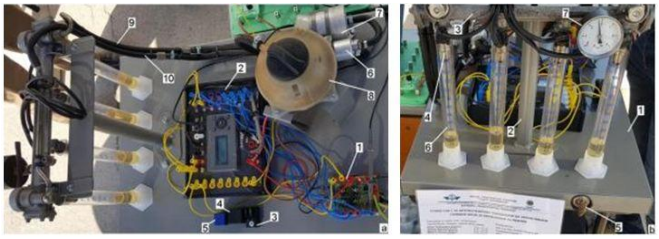

Fig. 2 *Common view of the test bench SAV-1 for automated management of the automotive gasoline fuel injectors: a) 1-control panel; 2-controller MI0245; 3-fuses; 4-fuel pump relay; 5-main relay; 6-fuel pump; 7-fuel filter; 8-fuel tank; 9-pump line; 10-return line b) 1-base plate; 2-fuel rail bar; 3-fuel rail; 4-fuel injector; 5-ignition key; 6-metering glass; 7-manometer*

3.Methodology

The EFMS100 equipment is connected to the test bench SAV-1. The fuel sensors 3 (fig.1) are connected to the pump line 9 and return line 10 (fig.2a). The fuel to use is gasoline, which is in the fuel tank 9. The gasoline is pumped by the fuel pump 6 and is pressurized in the fuel rail 3 (fig.2b). The gasoline pressure is maintained by the fuel pressure regulator in limits of 3-4 bar. The gauge 7 measures the pressure. The controller MI0245 2 (fig.2a) manages the fuel injectors 4 (fig.2b). The Flowcode 7 software develops the management program.

The management program determines the opening and closing time of the injectors, i.e. the injection duration and injection advance.

The metering glasses 6 are used to measure the fuel sprayed from the injectors. The metering glasses are an A class according to the DIN 12680. The quantity of sprayed fuel in the metering glasses is compared to the quantity registered by the EFMS100 system. The whole equipment is powered form the 12V battery or by an adaptor from the electric set.

The two fuel sensors are metering the fuel flow in the pump line and the return line. The measured values of the sensors are registered in the metering units and displayed on the display units. The difference between measured values is the real fuel quantity which is essential for the calibration. The static tuning, or calibration is carried on by the values from the pump line fuel sensor. In this case the test bench is set to pump mode, i.e. the regulator does not permit the fuel to the return line. The dynamic

tuning is carried on by the values from the two sensors, i.e. by the differential value of the sensors. The results from this tuning is object of another researching.

The static calibration is performed in the four modes, which have main automotive application. These modes are:

1) Continuous – all injectors are activated and produce continuous spraying;
2) Simultaneous – all injectors are pulse activated and produce pulse spaying;
3) Semi-sequential – the injectors are pulse activated in groups and produce group pulse spraying;
4) Sequential – the injectors are individual pulse activated and produce individual pulse spraying.

The pulse has three parameters:

1) ON_{time} – the time in which the injector is opened;
2) OFF_{time} – the time in which the injector is closed;
3) Duty cycle D:

$$D = \frac{ON_{time}}{ON_{time} + OFF_{time}}.100,\% \quad (1)$$

The timing of the ON_{time} and OFF_{time} are varying from 5 to 45 ms at the step of 5 ms, and D is varying from 10 to 90%. There are the following combinations, which are represented on the Table 1. These values are corresponding to the real injection automotive processes.

Table 1: *Timing combinations.*

ON_{time}, ms	OFF_{time}, ms	D, %
5	45	10
10	40	20
15	35	30
20	30	40
25	25	50
30	20	60
35	15	70
40	10	80
45	5	90

The quantity of fuel sprayed in the metering glasses is set to be 100 ml. After that, the test bench SAV-1 is paused and is performing the comparison between the sprayed and registered fuel quantity. Then is performed the EFMS100 adjustment if required. The adjustment is made by the EFMS100 menu, which gave the access to the parameter *PVR* – pulse/volume ratio. This parameter is calculated the by the formulae:

$$PVR = \frac{FPC}{Q_f}, \quad (2)$$

where *FPC* is the fuel flow pulse count, which is the number of revolutions of the flow sensor turbine to the measured fuel quantity; Q_f. – the measured fuel quantity.

Then the calculated *PVR* is set in the EFMS100 menu.

4.Results

After the performed experiments is obtained the following results, which are displayed in graphic diagrams. The fig.3 displays the fuel metering results during the Continuous mode. In this case the fuel injectors are spraying continuously. The characteristic shows equal dependence between metering glasses and calibrated EFMS100 system. The deviation of the experiment 3 is because of fuel flow fluctuations, which has chance character.

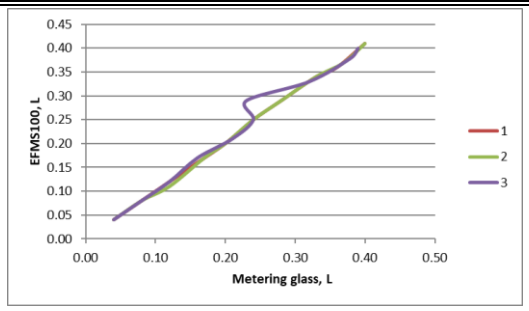

Fig.3 *Fuel flow metering characteristic at Continuous mode: 1,2,3-number of experiments*

At the next fig.4 is displayed the fuel flow characteristic during the Simultaneous mode. At this mode, the injectors work at varying the ON_{time} and OFF_{time} timing as mentioned above.

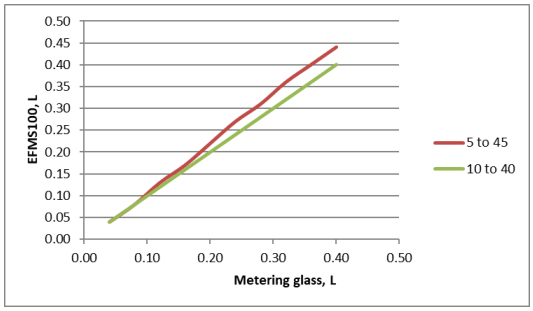

Fig.4 *Fuel flow metering characteristic at Simultaneous mode*

The remain combinations are the same with the second combination 10 to 40 ms.

The Semi-sequential mode is displayed on the fig.5. The timing of the ON_{time} and OFF_{time} is the same as previous Simultaneous mode. All the combination shows equal characteristic and are layered one above other.

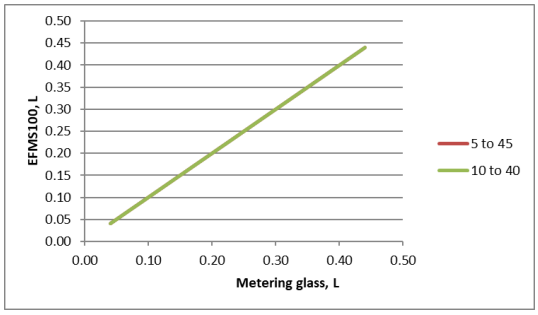

Fig.5 *Fuel flow metering characteristic at Semi-sequential mode*

The last and most modern automotive injection sequention is the Sequential mode. Its characteristic is shown on the fig.6 and the timing is the same.

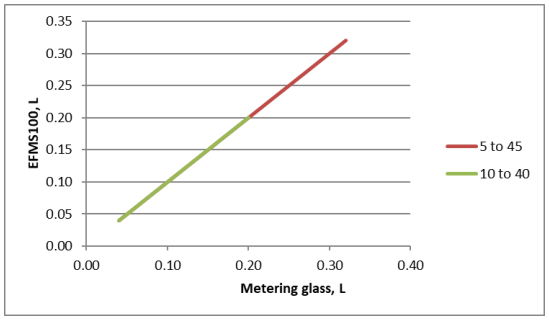

Fig.6 *Fuel flow metering characteristic at Sequential mode*

As can be seen, all the fuel flow characteristic has approximate dependence, which is essential to the static tuning, i.e. static calibration of the calibrated system.

5.Calibration

During the experiments at the previous point can be seen that the main difference is rendered at the little quantities of injected fuel, i.e. at the ON_{time} timing of 5 to 10 ms. To achieve the comparative characteristic of the calibration or calibration characteristic it is important to compare the *FPC* values with the fuel quantity values during the four modes. The values for the Continuous and Simultaneous mode is represented in the Table 2.

Table 2: *Comparative value for the Continuous and Simultaneous mode.*

Continuous		Simultaneous			
fuel, L	FPC	ON5ms, OFF45ms		ON10ms, OFF40ms	
		fuel, L	FPC	fuel, L	FPC
0.04	636	0.04	1411	0.04	975
0.08	1153	0.08	2721	0.08	1855
0.12	1770	0.12	4590	0.12	2729
0.16	2545	0.16	6008	0.16	3633
0.20	3134	0.20	7663	0.20	4502
0.24	3781	0.24	9323	0.24	5475
0.28	4425	0.28	10866	0.28	6361
0.33	5079	0.32	12352	0.32	7337
0.36	5656	0.36	13822	0.36	8172
0.40	6152	0.40	15168	0.40	9063

The values in the table and the remain values are represented on the fig.7. As was mentioned above the range of little fuel quantities is critical for the adjustment and calibration.

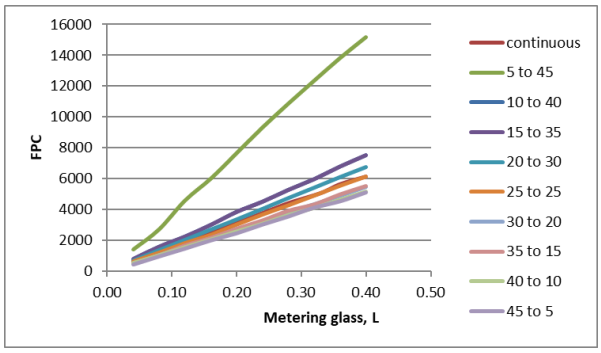

Fig.7 *Calibration characteristic at Continuous and Simultaneous mode*

The values for the Semi-sequential and Sequential mode is represented in the Table 3.

Table 3: *Comparative value for the Semi-sequential and Sequential mode.*

Semi-sequential				Sequential			
ON5ms, OFF45ms		ON10ms, OFF40ms		ON5ms, OFF45ms		ON10ms, OFF40ms	
fuel, L	FPC	fuel, L	FPC	fuel, L	FPC	fuel, L	FPC
0.04	2055	0.04	1340	0.04	2383	0.04	1783
0.08	4163	0.08	2604	0.10	6811	0.08	3783
0.18	9241	0.18	5626	0.20	13041	0.12	5895
0.30	15736	0.31	9808	0.28	18619	0.16	7970
0.20	7663	0.20	4502	0.32	22867	0.20	9914

The values in the table and the remain values are represented on the fig.8.

As it is shown on the fig.7 and fig.8, there is critical area in the range of little fuel quantities, i.e. at the little ON_{time} values. This area is more likely to be the reason for incorrect fuel flow measurements. So, the static calibration must be performed in this area.

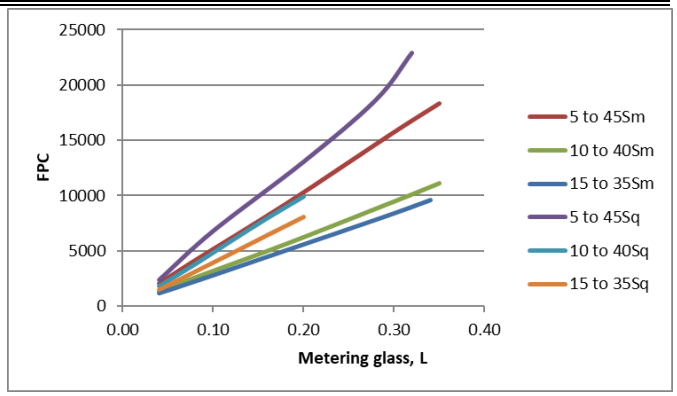

Fig.8 *Calibration characteristic at Semi-sequential and Sequential mode*

The correct calibration consists the following:

1) Setting up the timing to the minimal ON_{time} values (for example 5 ms)
2) Defining the control fuel quantity Q_f (for example 200 ml)
3) Performing the experiment
4) Comparing the values of sprayed fuel quantity Q_f by the metering glasses and by the display of calibrating system
5) If there is difference between the readings the parameter PVR must be update, according to below
6) Reading the values of sprayed fuel quantity Q_f by the metering glasses and the values of the parameter *FPC*.
7) Calculating the PVR parameter by the (2)
8) Setting up the updated PVR value in the menu of the calibrated system
9) Repeating the experiment and comparing the readings

After the correct calibration, the fuel metering system can be attached to the real HEV and can be made experiments to determine its fuel consumption during different driving modes in different areas. This will give the accurate evaluation of the HEV fuel efficiency.

Conclusion

The experimental calibration of the fuel metering system for the HEV fuel consumption is needful and important factor for the correct fuel metering.

Static tuning or calibration must made in the little fuel flow quantity modes to achieve the accurate tuning of calibrated system. Thus, the fuel consumption during idle mode of the HEV will be accurately define, moreover the idle mode is very common during the city traffic conditions.

Literature

[1] Slavcho Bozhkov, Boris Kirilov, Teodor Valev, Evelina Pircheva, Penko Bozhkov, Test Bench SAV-1 for Automated Management of the Automotive Gasoline Fuel Injectors, International Scientific Conference „MACHINERY AND CONSTRUCTION TECHNOLOGIES IN TRANSPORT" - 2018", Academic journal "Mechanics Transport Communication", ISSN 1312-3823 (print), ISSN 2367-6620 (online), volume 16, issue 3/3, 2018, article No 1676, pp.VI-36-VI-41, Todor Kableshkov University of Transport, Sofia, 2018 https://mtc-aj.com/library/1676_EN.pdf

[2] Иван Миленов, Славчо Божков, Георги Тонков, Особености в компановката и електрозадвижването на хибридни автомобили, Четвърта научна конференция с международно участие „Комуникации,

електрообзавеждане и информатика в транспорта – КЕИТ 2018", Научно списание "Механика, транспорт, комуникации" ISSN 1312-3823 (print), ISSN 2367-6620 (online), том 16, брой 3/2, 2018г., статия No 1716, стр.X-14-X-19, ВТУ «Тодор Каблешков», София, 2018 https://mtc-aj.com/library/1716.pdf

[3] Slavcho Bozhkov, Marian Mutafchiev, Ivan Milenov, Penko Bozhkov, M.I. Bichurin, R.V. Petrov. Method for determination of the hybrid electric vehicle energy efficiency in urban transportation // Вестн. Новг. гос. ун-та. Сер.: Технические науки. 2019. УДК 681.586.785, 2019, DOI: https://doi.org/10.34680/2076-8052.2019.4(116).4-8 http://www.novsu.ru/file/1575020

[4] http://www.enginemeter.com/site/

[5] Slavcho Bozhkov, Boris Kirilov, Teodor Valev, Evelina Pircheva, Penko Bozhkov, Test Bench SAV-1 for Automated Management of the Automotive Gasoline Fuel Injectors, International Scientific Conference „MACHINERY AND CONSTRUCTION TECHNOLOGIES IN TRANSPORT" - 2018", Academic journal "Mechanics Transport Communication", ISSN 1312-3823 (print), ISSN 2367-6620 (online), volume 16, issue 3/3, 2018, article No 1676, pp.VI-36-VI-41, Todor Kableshkov University of Transport, Sofia, 2018 https://mtc-aj.com/library/1676_EN.pdf

[6] http://www.matrixtsl.com

Investigation of the influence of fulleren-containing oils on tribotechnical characteristics

Derkach Oleksii[1], Kobets Anatolii[1], Aulin Viktor[3], Kabat Oleh[1,2], Makarenko Dmytro[1], Hrynkiv Andriy[3], Shchus Bogdan[1]

Dnipro State Agrarian and Economic University [1], Ukrainian State University of Chemical Technology [2], Central Ukrainian National Technical University [3] – Ukraine
e-mail: derkach_dsau@i.ua

Abstract: *The influence of fullerenes' soot concentration, which added to oil M10г2к on few tribotechnical characteristics «steel-steel» was investigated. It was found, that optimal volume of fullerene soot in the oil was 0,1% of the weight. At this level of concentration can be seen the lowest values of coefficient of friction – 0,045, and intense of linear wearing - $2,7\times10^{-9}$. Through optical investigation the participation of fullerene soot in surface forming mechanism and saturated with carbon was confirmed, it provided an increase in tribotechnical characteristics of the samples.*

KEYWORDS*: FULLERENE SOOT, OIL, CONCENTRATION, TRIBOTECHNICAL CHARACTERISTICS*

1. Introduction

One of directions of further progress in the engineering level of machines and mechanism lies in remarkable growth in their productivity without looses in products' quality, which are being launched or serviced. Obviously, it cannot be done without changing of their construction and improvement of materials [1], it's lead up to an increasing of intensity of the work rate in triboconjunctions [2]. Changing the design is a very effective means of improving the machines and mechanisms' productivity, but for its implementation it's necessary to spend a large number of human, intellectual and material resources, which are not always served as the optimal solutions. The growth of intensity of the operating mode of the main machines' joints and mechanisms lead to reducing in their reliability and longevity. Moreover, this issue connects mainly with friction assemblies, which are more sensitive to the effect of high levels of loads, velocities and temperatures, the growth of which is inevitable when the equipment is intensified [3, 4]. That's why an actual task is to rise up reliability and longevity of the tribology applications of machines and mechanisms, which are working under condition of the high loads, velocities and temperatures. Such task can be solved with aid to upgrading lubricants' facilities, which are being used in friction units. It will allow to decreasing in temperature load, friction and wear of working surfaces. It's well known, that there are at least three requirements to the oils, such as: removing from friction area wear debris, deduction of temperature load and coefficient of friction. There are another requirements to triboengineering, which are provided them with plenty number of additives, that were added to the oils. As follows, nowadays the starting conditions had been created in order to develop lubricants with high value of the lubricating properties; they could solve the problems with absolute restoration of working surface in triboengineering systems. One the way to increase oiliness is using modified additives, and also, fullerenes in any state [7].

2. Literature Review

Application of the fullerenes in the capacity of modifier of plastic lubricants and oils [8]. Although, with using carbonic microspheres as the fillers to oils [9]. In both cases, it would lead to decreasing in coefficient of friction and wear. Obviously, that application of the fullerenes in oils as the repening modifiers provides changing of friction character at the frictional engagement of steel parts with hope of triboengineering reactions in contact area [10]. It is allow to reduce significantly the friction and wear of details in machines' joints and mechanism, what assists the reliability and longevity to be risen. Received dependence of lubricating properties of oils, filled with fullerenes C_{60} from density of mineral base [11]. It was found, that application of fullerenes forward not only to reduce friction and wear-out of parts, which are in the frictional interaction, but to restore defective friction surfaces. It was found, that lower coefficient of friction and wear had provided due to rolling of specific nanoparticles [12]. It's mean, that decreasing in value of coefficient of friction was provided not even by sliding effect, but with aid of rolling of molecules and theirs groups on the operating points of surfaces. Consequently, it can be assumed, that due to fullerene's physical and chemical, they can influence on reducing in friction and tearing of details at the frictional interaction and in the condition of modified oils.

However, today the fullerenes are rather scare, expensive and used, as a rule in special machines. Industrial production of them is cheaper, cause to absence of development in this field at present stage. This is fundamental obstacle to their commonly use in machinery. That's why was found the necessity of investigation effective usage in fullerenes' mixtures and others, rather cheap components, such as thermically split graphite, in the function of modifier [13]. Modified oil was tested on the standard four ball machine, where positive tribological effect was defined. It is known, that other fullerene-containing materials, they are intermediates or borderline products, which were got with aid of synthesis of fair fullerenes. They are more available then others in the market. To such material as fullerene soot and fullerene crowd can be applied, they can be included in volume from 1 to 10% of fullerene's weight part [14]. Investigation of oils' properties, which were modified in so much that these materials it's still not enough. By the way, it was shown, that addition to the oils of fullerene crowds in volume of 5%, in which are 15…20 % of fullerenes C_{60}, it'd reduce tribological load in conjunction «steel-cooper» type [15]. As follows, positive effect at the application of fullerene soot, which was contained fullerenes що C_{60}, it was equal, as with applying extradite pure material C_{60}. The fullerenes can be implied in metallurgy at the exploitation of open-texture matrixes, also was found that friction mode had changed and characteristics of poromeric triboengineering systems had improved [16]. Described above results are created the starting condictions for investigation of influence of fullerene soot and on the tribosystems «steel-steel» type. Naturally, these materials can be in function of effective modifiers of oils. It's applied to commonly used oils, such as, for example, M10г2к. An actual task is defining the impact of FS on oils' lubricating properties, which are used in machines' and mechanisms' friction conjunctions commercially.

3. Materials and Methods

The main aim was to approve optimal volume of fullerene-containing oil with aid to studies of tribological properties of friction pair «steel-steel» at the application of fullerene.

To reach the goal, the next tasks were set:

- fullerene-containing oil through various volume of fullerene;
- to investigate tribilogical properties of friction pair «steel-steel» at the greasing by modified oil and determination of optimal fullerene-containing in it;

- to define the reason of changing of tribological properties of friction pair «steel-steel» at the greasing by fullerene-containing oil through investigation of friction surfaces'.

Objects and methods of investigation fullerene-containing oils on tribological characteristics of steel conjunctions.

In the function of basic material for investigation was chosen oil М10г2к, as the most widespread, and customer grade price, that was using numerous numbers of machines, like: large machines, lots of other means of transport and for special equipments, for instance, stationary generator. This oil is used in diesel, including, such as КамА3-740 and its' modifications. The main features of oils are presented in table 1.

Table 1: Some of the main features oil М10г2к

Parameter	Unit of measure	Value
Density at 20°C	g/sm³	0,9
Kinematic viscosity at 100°C	mm^2/s	11±0,5
Flash point	°C	220
Freezing point	°C	-18
Ash residue	%	1,15
Active elements (additives) per wt: - calcium - zink and phosphorous	%	 0,19 0,05
Additions from mechanical origin, less than or equal to	%	0,015

As modifier was chosen fullerene-containing material – a fullerene soot, as co-product of the synthesis of basic fullerenes C_{60}. To carry out the studies fullerene soot was used, that was given by Saint Petersburg State Institute of Technology.

The impact of fullerene soot on lubricating facilities by changing their tribological properties in friction area, which was working with these oils was defined. The investigation of properties was being conducted on the friction machine СМЦ-2 by scheme «disk-shoe» at the oil immersion. The load and rubbing speed at the experiment were 10 MPa and 1,3 m/s respectively. Each of experiments was being carried out among two hours and was repeated three times. The temperatures of modified oils were defining with aid of thermo couple D-301. Ruggedness of working surfaces (parameter *Ra*) was defined with aid of point contact follower 296 by standard methodology. In function of materials for friction pairs were used steel samples based on steel 45. The disks were heat treated to 42…45 HRC. Wearing surface roughness was bought up to Ra = 0,63 mkm.

The morphology of surfaces was studied with hope of scanning electron microscope (CEM) Hitachi S4800.

4. Experimental

According to our previous results [15], we expected to get decreasing in the main tribological parameters by optimal volume of fullerene soot in oil. To conduct teats the oils were prepared such as, modified in volume 0,1; 0,3 and 0,5% of the weight part in fullerene soot. Such levels of concentration were chosen in order to previous studies [17, 18].

The results of investigations of changing coefficient of friction in friction pair «steel-steel» type at the process of frictional engagement in the condition of basic and modified oils showed on the fig. 1.

In accordance to received results concentration dependences have growth character. It had been discovered, that in the area of modifiers' concentration FS 0,1 % could be seen dramatic reduce in coefficient of friction (fig.1), temperature (fig. 2) and remarkable – intensity of linear wear (fig. 3).

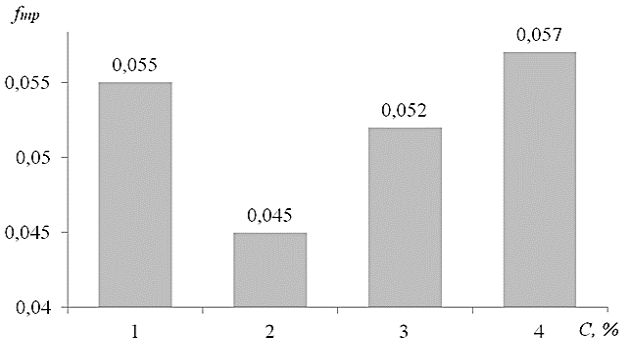

Fig. 1 *– The concentration dependence of coefficient of friction f_{mp} at the process of frictional engagement in the condition of basic and modified oils.*

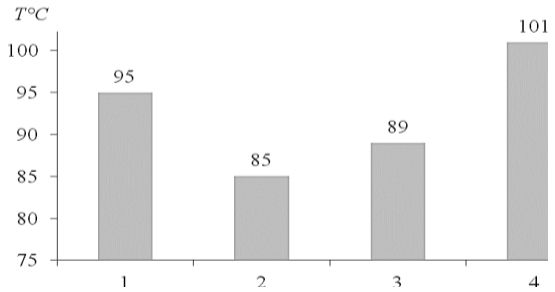

Fig. 2 *– Concentration dependence of the sample's temperature in friction area f_{mp} at the process of frictional engagement in the condition of basic and modified oils: 2 – 0,1 %; 3 – 0,3 %; 4 – 0,5 %.*

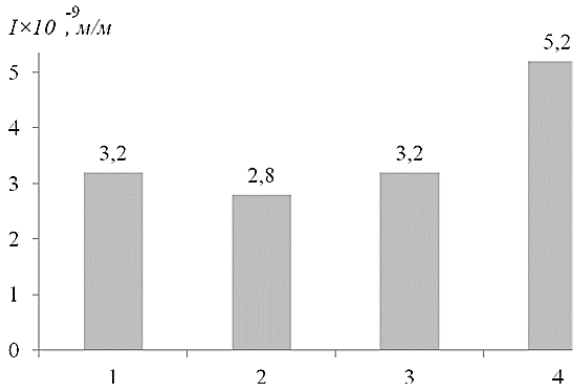

Fig. 3 *– Concentration dependence of the sample's linear wear L at the frictional engagement at the process of frictional engagement in the condition of basic and modified oils: 2 – 0,1 %; 3 – 0,3 %; 4 – 0,5 %*

Hear with reducing of these parameters is within 10-20% or less, than at the friction in non-modified oil. With increasing in weight part of fullerene soot in oil, all mentioned parameters are having steady growth. At the weight part of fullerene soot in oil even 0,5 % the value of the coefficient of friction f_{mp} has been exceed in basic variant.

It's known [19, 20], that fullerenes, even in small quantity are able to form the structure on the rubbing surface. It leads to creation of solid and flexible coat, which rise the tribological properties of friction pair, that we defined.

To finding out such coat on the friction surface after frictional engagement in oil, modified with FS, there was conducted an investigation on the subject surface roughness. It was determined by one the main parameters of roughness *Ra*. The results of tests are devoted on the fig. 4.

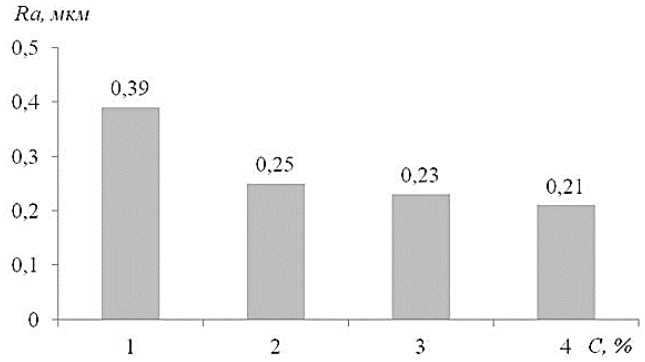

Fig. 4 *– Concentration dependence of roughness according to Ra of friction surface after frictional interaction in condition of basic and modified fullerene-containing oils: 2 – 0,1 %; 3 – 0,3 %; 4 – 0,5 %.*

It was set, that immerse of fullerene soot in oil provides decreasing in wearing roughness of surfaces. By the way, in this particular case they are accurate propulsions of these parameters: with increasing in weight part of fullerene soot in oil, roughness *Ra* is going back. In general ii was found reducing in roughness within volumes of 36…46 % in comparison with surface's roughness, which was got from clear oil. On the fig. 5 is showed proposed scheme of rubbing surfaces' profiles after frictional engagement in base and modified oils.

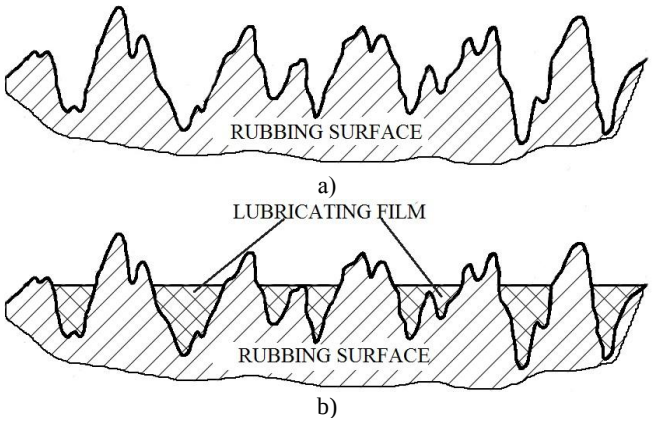

Fig. 5 *– Proposed scheme of rubbing surfaces profiles after frictional engagement in condition of base (a) and modified (b) oils.*

Existence of lubricating film on the surfaces also can be confirmed by micrometric shots of them after frictional engagement in condition of base and modified oils (Fig. 6).

While zooming to × 2500 times, there were found an intensive filling of micro depressions (Fig. 7, *a*) and forming superficial formations by the components of fullerene soot.

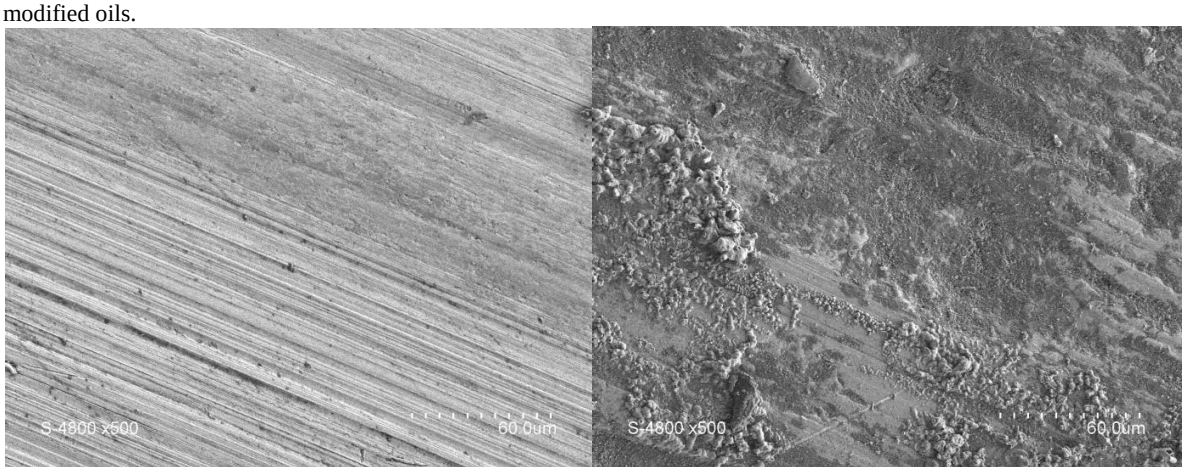

Fig. 6 *– Micrometrical shots of rubbing surfaces after frictional engagement in condition of (a) base and (б) modified oils. Picture CEM, × 500 times.*

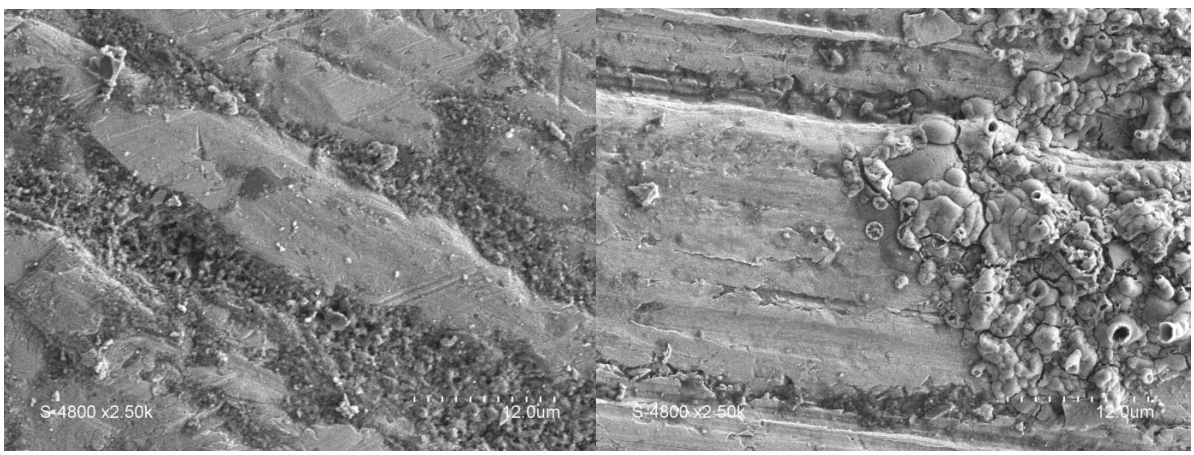

Fig. 7 *– Micrometric shots of the friction surfaces after frictional interaction in the condition of modified oil. Picture CEM, × 2500 times*

5. Results and discussion

It was known, that using fullerene-containing oils should improve friction mode and reduce wear of metal tribological distinction. Generally, such suppose was absolutely appropriate.

Influence of fullerenes' weight part on coefficient of friction, temperature and intensity of linear wear. Actually, at the addition fullerene soot into the oil in volume till 0,1 % of weight can be seen improvement of tribological properties of friction pair, that is explained by changing in character of friction due to contents of FS in the structure. By contrast, in case of increasing the weight part of fullerene soot in the oil, the coefficient of friction (picture1), temperature in contact area (picture 2) and intensity of linear wear (picture 3) are on the rise. As can be assumed, that at the increasing

in volume of FS, the soot shall be has preference, as a matrix, which contains physical carbon and rests of fullerenes' synthesis. These products are making impossible to roll-out of fullerene molecules groups on the working surface. In fact, friction shift plays a valuable role. Here can be made a hypothesis, that shows how at the small quantity of FS is taking place carbonation of working surface, and in case of its end or numerous volume of carbon, tribological properties will be disimpoved.

Influence of weight part of FS on surfaces' roughness. Process of growth down of working surface roughness *Ra* is justified supposes as for forming lubricating film on the rubbing surfaces, it is filling out microroughnesses, that declining the level of roughness after frictional interaction in condition of modified oil. Despite of this, in such conditions appears a smooth finish on the rubbing surface with aid of fullerene soot's products. As supposed, the layers of film would be within defined values. It allows to downturn the parameters of vibration and noise in tribological distinctions.

As can be seen micrometric shots, working surfaces, which are gotten after frictional interaction in condition of base and modified oils they have a significant differences. So, on the surface, is performed on the picture 6, *a*, are seeing in microroughnesses without any notable additives and inclusions. And surface (picture 6, *б*) is covered with lubricating film, and it is key reason, which influence on reducing friction and wear of friction pair at the friction in modified oil. The surfaces have different structures; there are superposition and concentration of fullerene soot. The difference between morphology of created coats should be noted (picture 7). Basically, these micro parcels are fullerene-containing materials, what has lead to positive effect. They are concentrated in dimples of microroughnesses, and it's creating solid lays of material, substantial, may be, fixed by chemical means on the rubbing surface. On the picture 7, *b* can be seen textual features; they are creating and developing with aid of tribochemical reactions, which are taking place at the friction. At the increasing of weight part of FS in oil such layers lead to negative consequence – force of moving FS molecules is growing, that is the reason of growth values of coefficient of friction f_{mp}, temperature in contact zone *T* and wear *I*. So, on the rubbing surface (picture 7, *a*) can be seen how unevenness of profile are filled with FS.

6. Conclusion

It was studied the impact of weight part of fullerenes in oil on the subject of tribological properties in tribological conjunctions «steel-steel» type and it was found optimal volume of modifier.

In conclusion, implementation of fullerene soot into the oil in optimal volume 0,1 % of its weight provided decreasing in: coefficient of friction to - 19%; temperature in contact area to - 11%; intense of linear wearing to - 13%; Wearing surface roughnesses to - 36%.

According to research, which was done on CEM it had found, that on the rubbing surfaces at the frictional engagement in condition of modified oil with added fullerene soot, it is taking place in process of forming the film, which is changing character of friction, and it's contribute to improvement of triboengineering characteristics of the metal samples, which are made from steel 45.

It was deeply recommended to apply oil М10г2к industrially, which has been modified with fullerene soot in volume 0,1 % of the weight.

7. References

[1] Mironova, D.Y. (2015). Sovremennye tendencii razvitiya nauki i tekhniki i marketing innovacij. SPb: Universitet ITMO, 83.

[2] Bogolyubov, A. N. (2017) Teoriya mekhanizmov i mashin v istoricheskom razvitii ee idej. Moskva: LENAND, 466.

[3] Garkunov, D.N. (2002) Tribotekhnika. Konstruirovanie, izgotovlenie i ehkspluataciya mashin. Moskva: Izdatel'stvo MSKHA, 632.

[4] Frolov, K.V. (2008) Sovremennaya tribologiya. Itogi i perspektiva. Moskva: Izdatel'stvo UKI, 480.

[5] Breki, A.D., Medvedeva, V.V. (2016) ZHidkie i konsistentnye smazochnye kompozicionnye materialy, soderzhashchie dispersnye chasticy gidrosilikatov magniya, dlya uzlov treniya upravlyaemyh sistem. Tula: Izd-vo TulGU, 166.

[6] Myshkin, N.K., Petrokovec, M.I. (2007) Trenie, smazka, iznos. Fizicheskie osnovy i tekhnicheskie prilozheniya tribologii. Moskva: FIZMATLIT, 368.

[7] Baoyong, L., Hongguang L. (2016) Alkylated fullerene as lubricant additive in paraffin oil for steel/steel contacts. Fullerenes Nanotubes and Carbon Nanostructures, 24, 712-719. https://doi.org/10.1080/1536383X.2016.1231178.

[8] Wu, Y.Y., Tsui, W.C., Liu T.C. (2007). Experimental analysis of tribological properties of lubricating oils with nanoparticle additives. Wear, 262, 819-825. https://doi.org/10.1016/j.wear.2006.08.021.

[9] Alazemi, A. A., Etacheri, V., Dysart, A. D., Stacke, L.-E., Pol, V. G., Sadeghi F. (2015). Ultrasmooth Submicrometer Carbon Spheres as Lubricant Additives for Friction and Wear Reduction. ACS Appl. Mater. Interfaces, 7, 5514-5521. DOI: 10.1021/acsami.5b00099.

[10] Erdemir, A., Martin, J.-M. (2007) Superlubricity. Amsterdam: Elsevier, 499.

[11] Ku, B.-C., Han, Y.-C., Lee, J.-E., Lee, J.-K., Park, S.-H., Hwang, Y.-J. (2010). Tribological effects of fullerene (C60) nanoparticles added in mineral lubricants according to its viscosity. International Journal of Precision Engineering and Manufacturing, 11(4), 607-611. DOI 10.1007/s12541-010-0070-8

[12] Rapoport, L., Nepomnyashchy, O., Verdyan, A., Popovitz-Biro, R., Volovik, Y., Ittah, B. (2004). Polymer Nanocomposites with Fullerene-like Solid Lubricant. Advanced Engineering Materials, 6(1-2), 44-48.

DOI 10.1002/adem.200300512.

[13] Yoshimoto, S., Amano, J., Miura, K. (2010). Synthesis of a fullerene/expanded graphite composite and its lubricating properties. Journal of Materials Science, 45(7), 1955-1962. DOI 10.1007/s10853-009-4187-z.

[14] Gruzinskaya, E.A., Keskinov, V.A., Keskinova, M.V., Selinov, K.N., CHarikov, N.A. (2012). Fullerenovaya sazha ehlektrodugovogo sinteza, 3, 83-90.

[15] Kireyenko, O.F., Ginzburg, B. M., Bulatov, V.P. (2002). Fullerene black as an antifriction and antiwear additive to lubricating oils. Journal of Friction and Wear, 23(3), 64-68.

[16] Rapoport, L., Lvovsky, M., Lapsker, I., Leshchinsky, V., Volovik, Y., Feldman, Y., Margolin, A., Rosentsveig, R., Tenne, R. (2001). Slow Release of Fullerene-like WS_2 Nanoparticles from Fe-Ni Graphite Matrix: A Self-Lubricating Nanocomposite. Nano Letters, 1(3), 137-140. DOI: 10.1021/nl005516v.

[17] Derkach, O.D., Burya, O.I., Harchenko, B.G. (2011). Zastosuvannya geomodifikatoriv dlya poverhon' tertya pri tekhnichnij ekspluataciï sil's'kogospodars'koï tekhniki. Visnik HNTUSG im. Petra Vasilenka, 109, 199-203.

[18] Derkach, O.D., Guba, M.I., Kabat, O.S. (2013). Obrruntuvannya parametriv fulerenovmisnih oliv. Visnik HNTUSG im. Petra Vasilenka, 134, 172-179.

[19] Kumar, N., Kozakov, A. T., Kolesnikov, V. I., Sidashov, A. V. (2017). Improving the lubricating properties of 10W40 oil using oxidized graphite additives. Journal of Friction and Wear, 38, 349-354. https://doi.org/10.3103/S1068366617050051.

[20] Shakirullah, M, Ahmad Im., Arsala Khan M., Ishaq M., Mohammad Saeed H. (2006). Spent Lubricating Oil Residues as New Precursors for Carbon. Fullerenes, Nanotubes and Carbon Nanostructures, 14, 39-48. https://doi.org/10.1080/15363830500538615.